Scientific Research and Essays Vol. 6(12), pp. 2525-2549, 18 June, 2011
Available online at http://www.academicjournals.org/SRE
ISSN 1992-2248 ©2011 Academic Journals

Full Length Research Paper

Axial-flux permanent-magnet machine modeling, design, simulation and analysis

A. Mahmoudi*, N. A. Rahim and W. P. Hew

Electrical Engineering Department, University of Malaya, Kuala Lumpur, Malaysia.

Accepted 19 May, 2011

Axial-flux permanent-magnet machines today are important technology in many applications, where they are an alternative to radial-flux permanent-magnet machines. Reviewed here are technology status and advances/trends in axial-flux permanent-magnet machines, in aspects of construction, features, modeling, simulation, analysis, and design procedure. Potential applications and future trends are also discussed.

Key words: Axial-flux permanent-magnet machines, finite-element analysis.

INTRODUCTION

Axial-flux permanent-magnet (AFPM) machines have many unique features. For being permanent magnet, they usually are more efficient, as field excitation losses are eliminated, reducing rotor losses significantly. Machine efficiency is thus greatly improved, and higher power density achieved. Axial-flux construction has less core material, so, high torque-to-weight ratio. Also, AFPM machines have thin magnets, so are smaller than radial-flux counterparts. AFPM machine size and shape are important features in applications where space is limited, so compatibility is crucial. The noise and vibration they produce are less than those of conventional machines. Their air gaps are planar and easily adjustable. Also, direction of main air-gap can be varied, so derivation of various discrete topologies is possible (Sitapati and Krishnan, 2001). These benefits give AFPM machines advantages over conventional machines, in various applications. Published literatures on AFPM machines contain AFPM-related issues such as machine modeling, analysis and design. Comprehensive review of AFPM structures, modeling, simulation, analysis, design procedure and applications are attempted by this paper.

Subsequently, the study discusses various AFPM machine structures, advantages, and issues specific to each configuration, after which it reviews AFPM machines capable of flux weakening. Furthermore, it reviews points of sizing equation, modeling and simulation, and then it reviews diverse aspects of analysis, such as cogging torque, thermal and structural. More so, the study describes the design procedure of an AFPM machine as a multi-dimensional optimization problem to maximize the efficiency within constraints. Finally, the study suggests and presents potential applications, as well as future trends.

Axial-flux permanent-magnet machine construction

AFPM machines were first introduced in late 70s and early 80s (Campbell, 1975; Leung and Chan, 1980; Weh et al., 1984). Growing interest in AFPM machines in several applications due to their high torque-to-weight ratio and efficiency as an alternative to conventional radial-flux machines was significant in the last decade. Basically, each radial-flux-machine type has its corresponding axial-flux version (Cavagnino et al., 2002). Practical categorizations are permanent-magnet DC commutator, permanent-magnet brushless DC, or synchronous AC. DC brushless and AC synchronous machines are equal in structure but differ in operation principle. EMF waveform generated by DC brushless is

*Corresponding author. E-mail: amaminmahmoudi@gmail.com. Tel: +60136778050. Fax: 03-7967 5317.

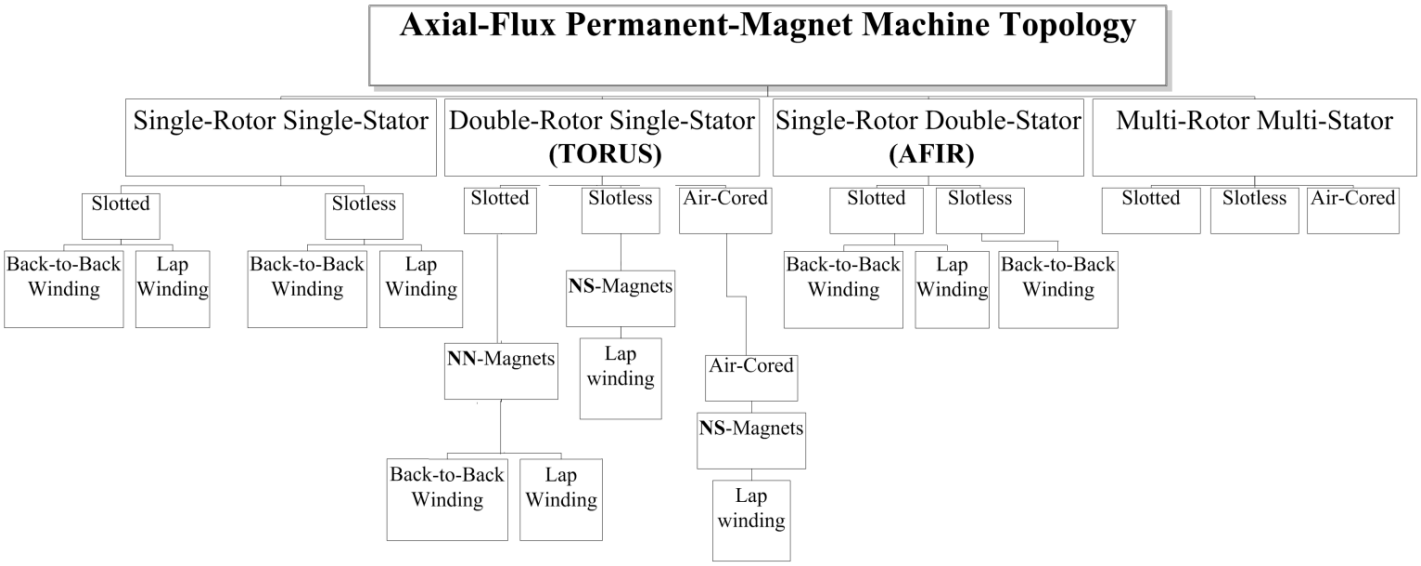

Figure 1. Various topologies of AFPM machines and their winding configurations.

trapezoidal. In AC synchronous it is sinusoidal. In construction, brushless AFPM can be single-sided or double-sided, with or without armature slots, with or without armature core, with internal or external permanent-magnet rotors, with surface-mounted or interior permanent-magnet, and as single-stage or multi-stage (Gieras et al., 2008). Figure 1 shows various AFPM topologies and their winding configurations. Subsequently, the study focuses on AFPM machines of various rotor and stator configurations.

Single-rotor single-stator axial-flux permanent-magnet

Figure 2 is basic and simplest-structure of AFPM machine; single rotor, single stator (Cheng-Tsung et al., 2003; Jang and Chang, 2002; Liu and Lee, 2006; Patterson and Spee, 1995; Zhang et al. 1997). It is subject to unbalanced axial force between rotor and stator, so, unlike structures with balanced axial forces, it requires more-complex bearing arrangements and thicker rotor disk (Chan, 1987; Platt, 1989). The magnetic force may twist the structure very easily. With slotless stator, axial force is less, as the force is exerted on iron, rather than on copper, windings (Campbell et al., 1981).

Double-rotor single-stator axial-flux permanent-magnet

Figure 3 is TORUS, a double-rotor single-stator AFPM machine. Its phase coils wound around the slotted stator (Caricchi et al., 1998, 1999; Muljadi et al., 1999; Profumo et al, 1997) or the slotless stator (Chalmers et al., 1999; Ficheux et al., 2001; Jensen at al., 1992; Spooner and Chalmers, 1992). Slotless-stator TORUS-type AFPM machine was first introduced in the late 1980s (Spooner and Chalmers, 1988). Slotted and slotless differ in the existence of slots in one, and in the type of winding in each. For increased robustness and better heat dissipation of conductor, portions between air-gap windings in slotless are filled with epoxy resin (Soderlund et al., 1996). Leakage and mutual inductance in slotless air-gap windings are lower, and effects due to slots, that is, flux ripple, cogging torque, high-frequency rotor losses and stator teeth, are eliminated (Caricchi et al., 2004). Windings in radial direction are used for torque production. In slotless, end windings are short, so, less copper losses, and better heat-dissipation of conductor (Aydin et al. 2001). Variations may be found in rotor magnet arrangement, which affects main flux path in rotor, in stator, and possibly in winding. In TORUS topology, main flux may flow axially through stator or circumferentially in stator yoke (Surong et al. 2001). Figure 4 shows possible flux paths. Figures 4a and b respectively relate to North-north and North-south magnet arrangements. Both structures show tangential Lorentz forces affecting phase-A coils. The structures are identical except for stator-yoke thickness and winding arrangement.

North-north (NN) structure has its phase winding wound around stator core, giving short end-windings (back-to-back windings) in both the axial and the radial directions of the machine (Parviainen, 2005). Very short end-windings reduce copper losses, but main flux has to flow

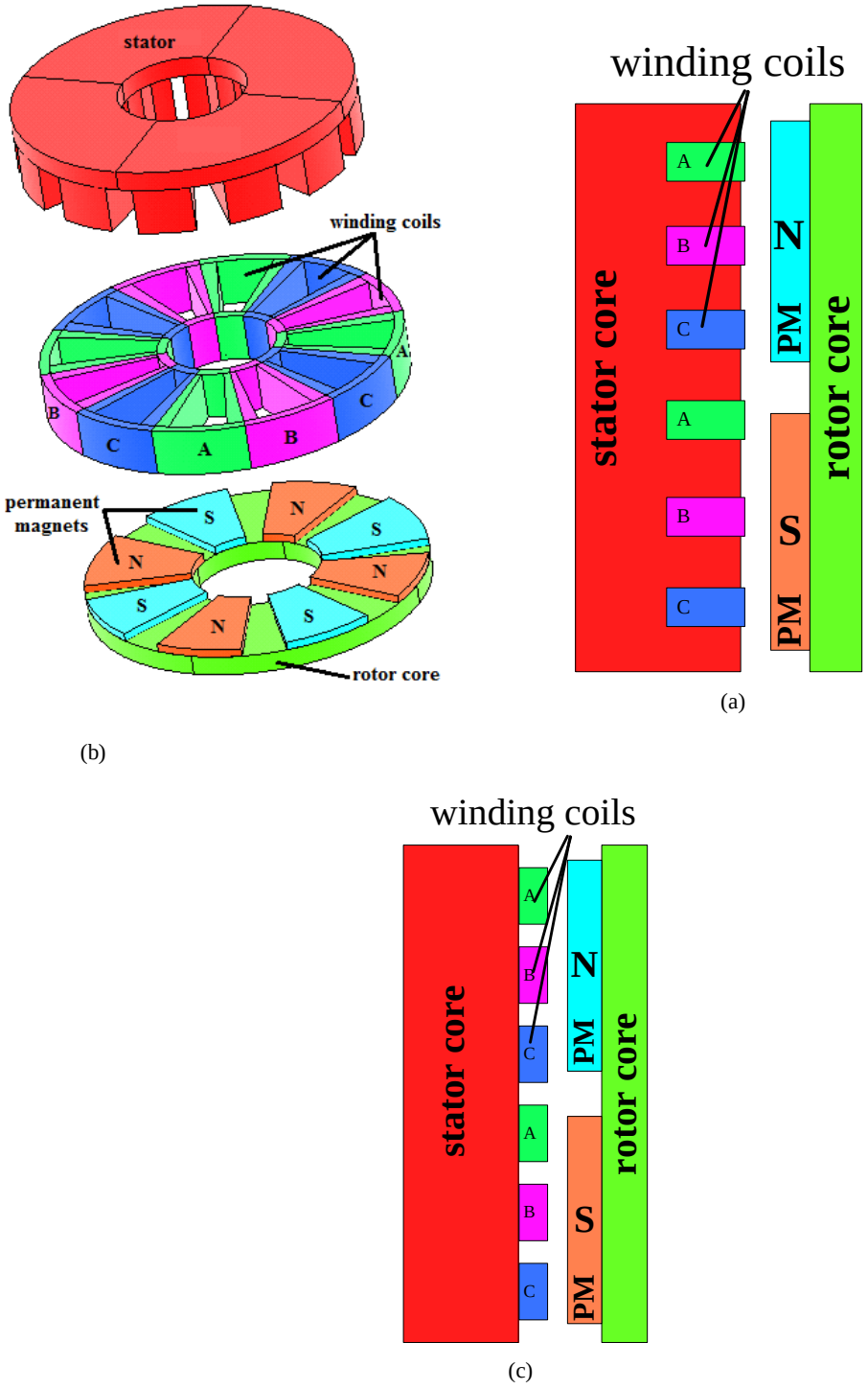

Figure 2. Construction of single-sided AFPM machine, a) 3D-view of a single-sided AFPM machine; b) slotted-stator single-sided AFPM machine and c) slotless-stator single-sided AFPM machine.

circumferentially along the stator core, so a thick stator yoke is required, for summation of flux entering stator from both rotors, the summation in turn increasing iron losses and lengthens end-windings. Owing to its flux direction, the machine could be thought of as a combination of two independent halves. North-south (NS)

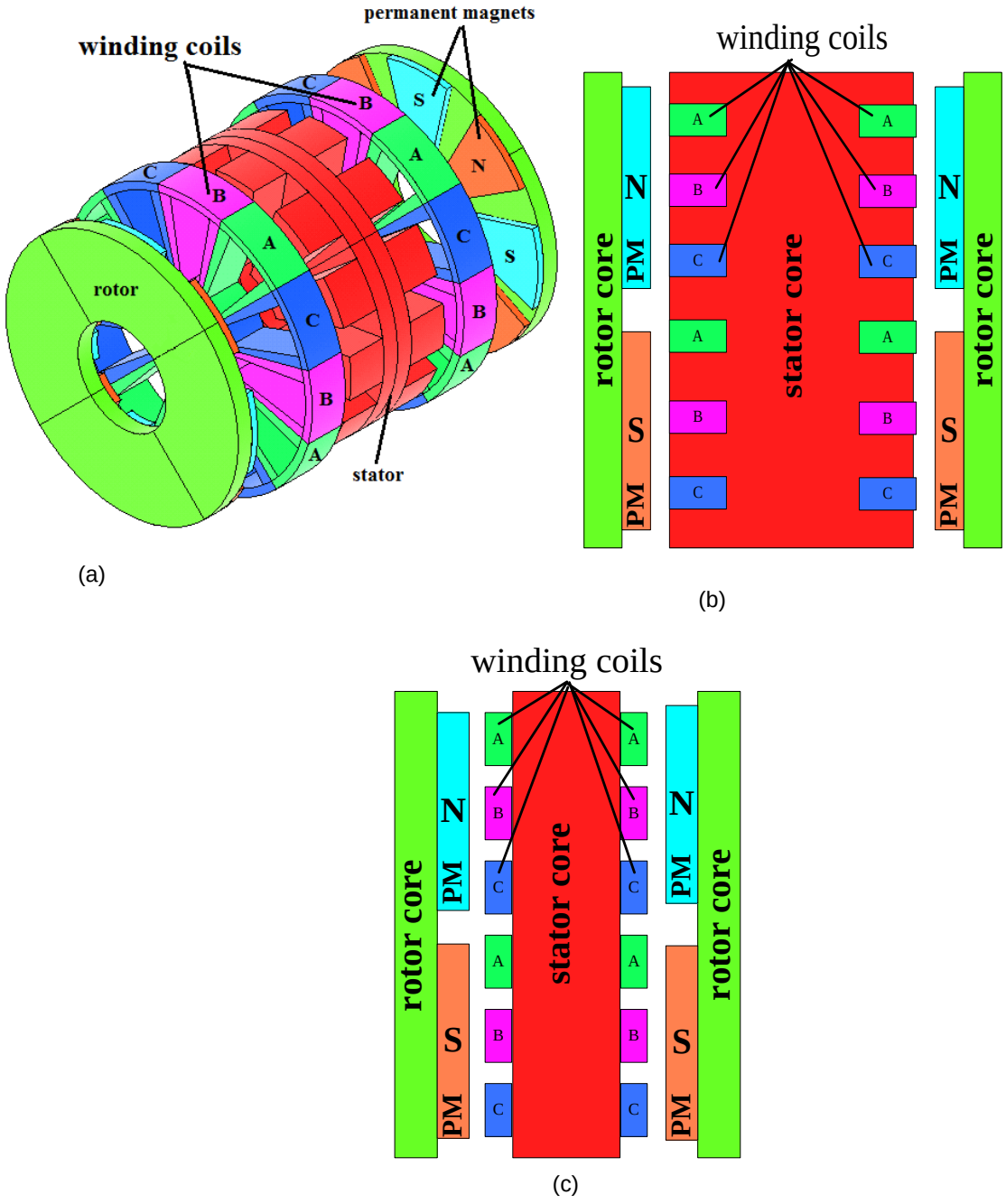

Figure 3. Single-stator double-rotor AFPM machine; (a) 3D view of a TORUS machine; (b) slotted stator TORUS AFPM machine and (c) slotless stator TORUS AFPM machine.

structure has main flux flowing axially through stator, so in principle, stator yoke is unnecessary (Woolmer and McCulloch, 2006). Iron losses are thus reduced, but lap windings are needed to produce torque (Locment et al., 2006; Takano et al., 1992). Lap windings lengthen end-windings, which again increase copper losses. External diameter of machine also increases. NN structure thus has less copper losses and smaller external diameter, but more iron losses and longer axial. To produce torque, either end winding or lap winding is used in NN structure, but only lap winding is used in NS structure. Another TORUS machine is coreless AFPM machine (Figure 5) (Bumby et al., 2005; El-Hasan et al., 2000; Hosseini et al., 2008; Kamper et al., 2008; Rossouw, 2009; Sadeghierad et al., 2009, 2009). Its main feature is elimination of stator yoke, as in NS TORUS main flux

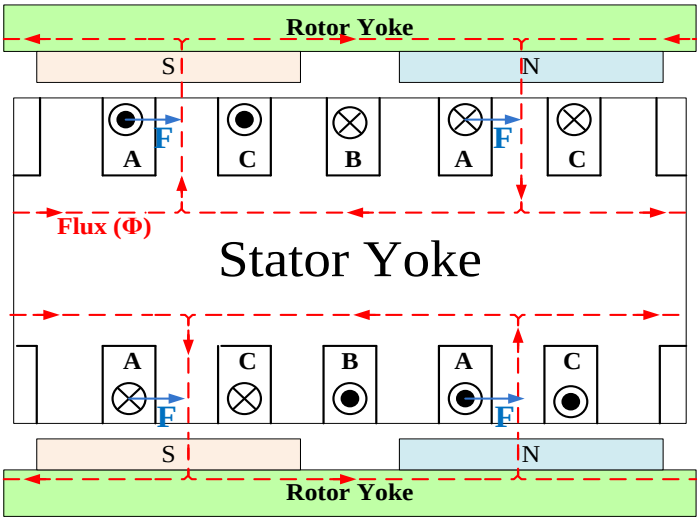

(a)

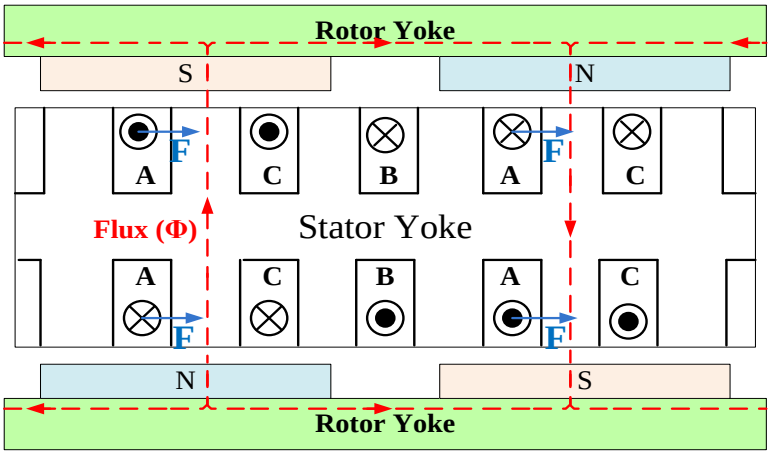

(b)

Figure 4. Flux paths in 2D plane for slotted stator of single-stator double-rotor AFPM machine; (a) North-north magnet arrangement and (b) North-south magnet arrangement.

flows from one rotor to another rather than travels circumferentially along stator core.

The stator has windings only, and the rotor has surface magnet as in other AFPM machines. This type of AFPM machine is efficient as there are no iron losses (Caricchi et al., 1998; Lombard et al., 1999).

Single-rotor double-stator axial-flux permanent-magnet

Figure 6 is a single-rotor double-stator AFPM machine called an axial-flux interior-rotor (AFIR) machine, constructed in slotted, or slotless, stator structure (Platt, 1989; Gieras and Wing, 2002; Parviainen and Pyrhönen, 2004). Its rotor structure differs from that of TORUS, and its permanent magnets can be located on rotor-disk surface or inside rotor disk. Main flux thus flows axially through rotor disk or circumferentially along rotor disk. Also, both arrangements may be used to build a single-stator single-rotor structure, but the main flux flow is always circumferential along rotor disk. Figure 7 shows in 2D plane, flux paths for a double-stator single-rotor structure of an AFPM machine. Surface-mounted structure (Figure 7a) has a very thin rotor, especially if the magnets had been installed inside a non- ferromagnetic

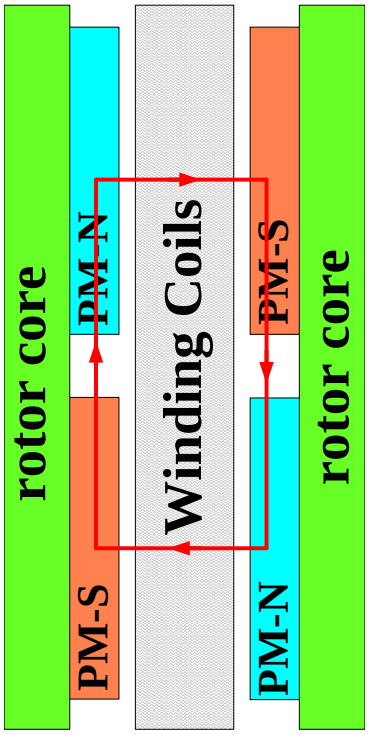

Figure 5. Coreless axial-flux permanent-magnet machine.

rotor core. When permanent-magnets are buried into the rotor disk, much thicker rotor disk is required (Figure 7b), consequently reducing machine power density, though structure of machine stator remains as it had been. Leakage flux in magnet ends is higher than the one in surface-mounted structure, as the magnets are surrounded by ferromagnetic material (Aydin et al., 2006). Constant magnet thickness and magnetization along machine radius may cause excessive saturation in inner-radius rotor core, because depending on machine inner diameter and pole pairs, inner radius of the permanent magnets may be very close to each other (Marignetti et al., 2010). Flux density on the outer radius is much less, causing non-constant flux-density distribution in air-gap along machine radius. Further comparing of surface-mounted structure with buried structure: armature reaction is higher in buried structure than in surface-mounted, as permanent magnets in surface-mounted configuration act almost as air and thus form long air-gap (Liu et al., 2004).

An advantage of buried structure is its better protection of magnets against mechanical impact, wear and corrosion. AFIR structure, whose rotor is located between stators, is simpler, as there is more space for windings (Caricchi et al., 1995). End windings of AFIR machines are relatively long owing to winding parts used for torque production being on stator-inner facing rotor, so, higher copper losses (Cavagnino et al., 2000). Copper losses in AFIR slotted machines are lower than those of their slotless counterpart, because AFIR end-windings are short (due to short-pitched winding). Also, inductance of AFIR machine is larger than that of equivalent TORUS machine. AFIR machine leakage-flux from non-torque-producing side links iron parts not appropriately associated with machine. For buried-magnet structure, a modular rotor-pole construction including layers of ferromagnetic and non-ferromagnetic materials may reduce armature reaction. Figure 8 shows such rotor structure. Non-ferromagnetic bridges between ferromagnetic layers increase armature field lines, so, with rotor pole of ferromagnetic material only, armature field is decreased. In the proposed structure, each stator teeth is supplied with approximately the same magnetic flux; the excitation field is thus virtually constant. Slits arranged between the ferromagnetic bridges diminish leakage fluxes in magnet ends (Weh et al., 1984). In AFIR structure, another rotor-pole construction is possible (Figure 9). It does not use steel disk in the rotor because main flux does not travel in rotor.

Non-magnetic material fills spaces between magnets and together with axially-magnetized fan-shaped permanent magnets makes the rotor rigid. AFIR construction has very high power-to-inertia ratio as its rotor lacks iron, so AFIR structure is preferred in applications needing small inertia.

Multi-rotor multi-stator AFPM

Several machines lined up on the same shaft form more-complex arrangements, also, multi-stage AFPM machine. Considering produced torque is a function of AFPM machine's outer diameter, in the case of limited outer diameter, the desired electromagnetic torque can be achieved by multi-stage arrangement. Such machines may be considered for ship propulsion (Caricchi et al., 1995), pump (Caricchi et al., 1998), high-speed permanent-magnet generator (El-Hasan et al., 2000), and research (Anyuan et al., 2010). Compared with multiple-stator multiple-rotor radial-flux permanent-magnet (RFPM) machines, multi-stage AFPM machines are more easily assembled because their air-gap surface stays constant (RFPM machine's surface gets smaller). Multi-stage AFPM machines generally have N stators and N + 1 rotor discs (N the number of stages or of stators). The rotors share a mechanical shaft. Stator winding can be parallel connected or serial connected. Rotor core is for outer rotor only, providing the main-flux path, so must be chosen carefully. Figure 10 is a multi-stage AFPM machine, whose N = 2. Multi-stage AFPM machines are not widely found in literatures. Whether TORUS or AFIR structure, AFPM machines can be multi-stage, with slotted or slotless stator, including NN or NS

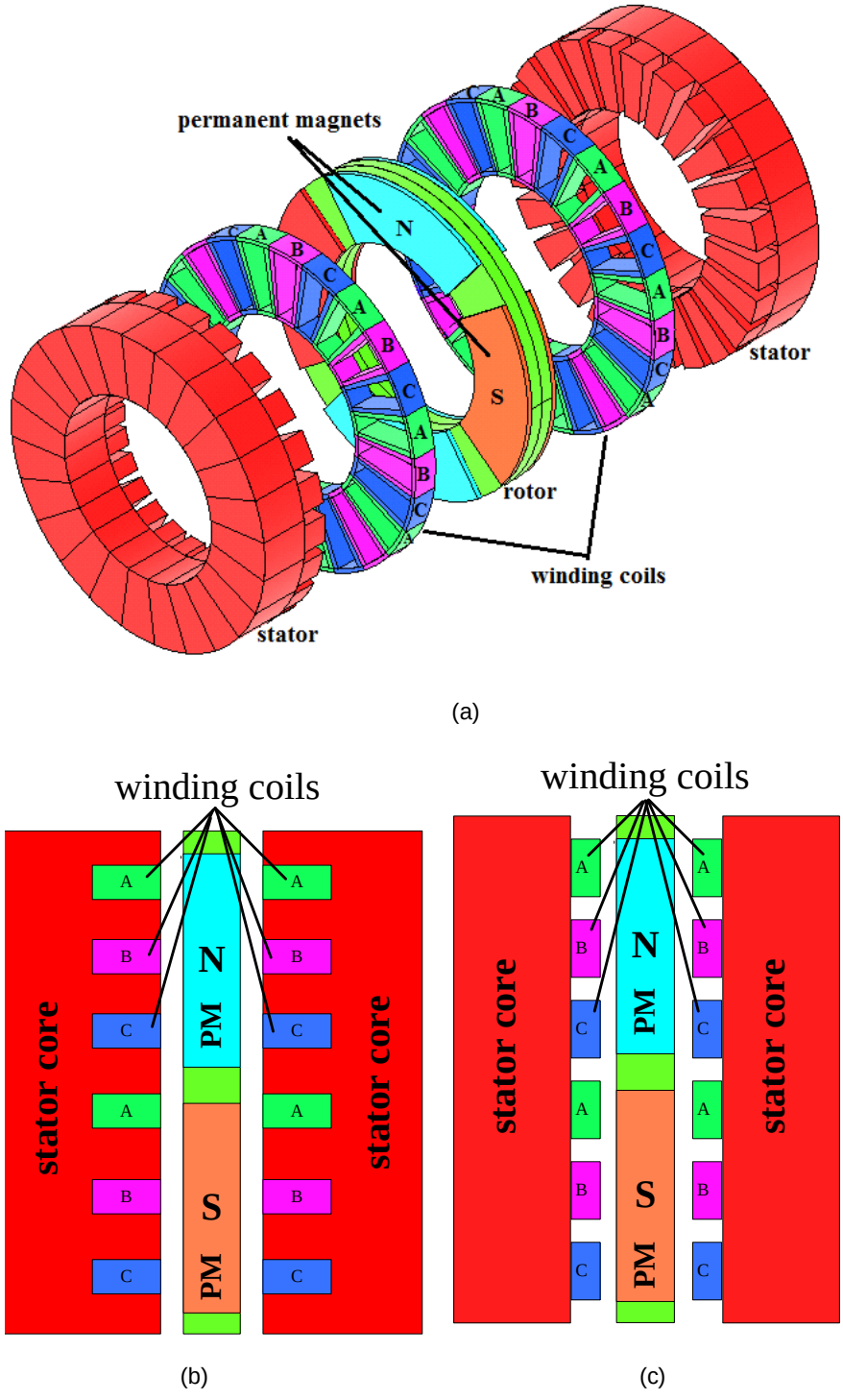

Figure 6. Double-stator single-rotor AFPM machine; (a) 3D view of an AFIR machine; (b) slotted stator AFIR permanent-magnet machine and (c) slotless stator AFIR permanent-magnet machine.

topologies. Advantages and disadvantages of each construction are similar to those of relevant preceding structures.

A multi-stage AFPM machine can be built with multiple rotors and ironless armature windings (Jee, 2008), in which case magnetic flux travels through machine axis,

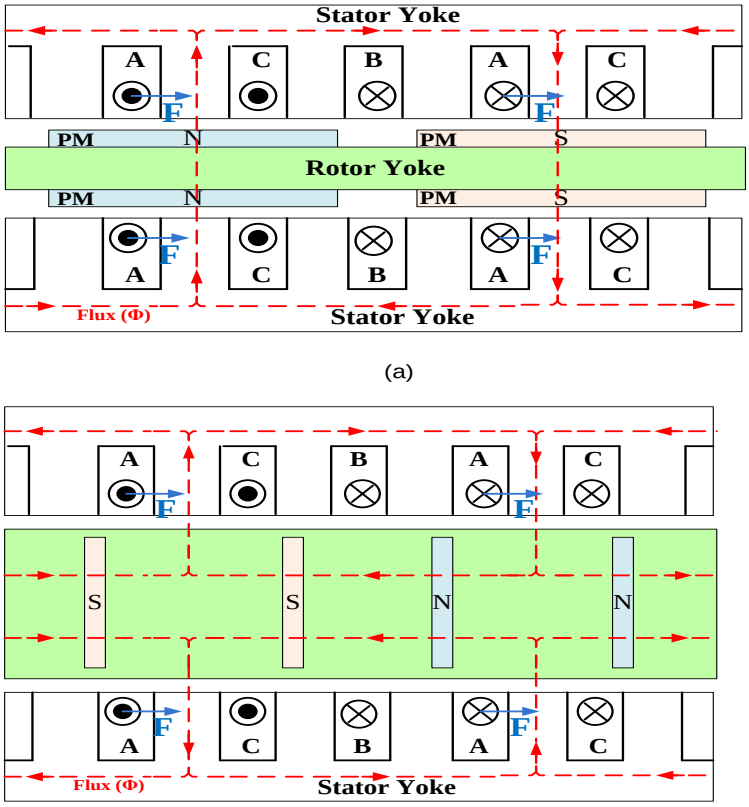

Figure 7. Flux paths in 2D plane for a double-stator single-rotor structure of an AFPM machine; (a) surface permanent-magnet and (b) buried permanent-magnet.

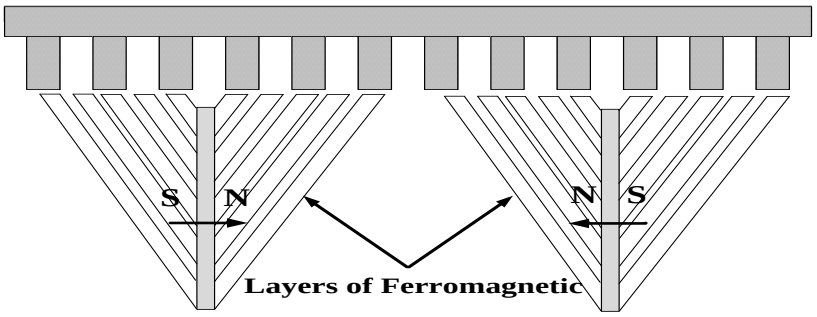

Figure 8. Rotor-pole structure capable of reducing armature reaction.

from one end to another (Figure 11).

Axial-flux permanent-magnet machine capable of field-weakening

Flux-weakening had not been available in AFPM machines. Achieving flux-weakening simply and without negative current injection effects is aimed for, so, AFPM machine designers have for years been interested in new configurations (Boules, 1985; Jahns, 1987; Sebastiangordon and Slemon, 1987). Solutions to the problem exist (Aydin et al., 2010; Hsu, 2000; Liang and Miller, 2002; Lipo and Aydin, 2004; Profumo et al., 1998,

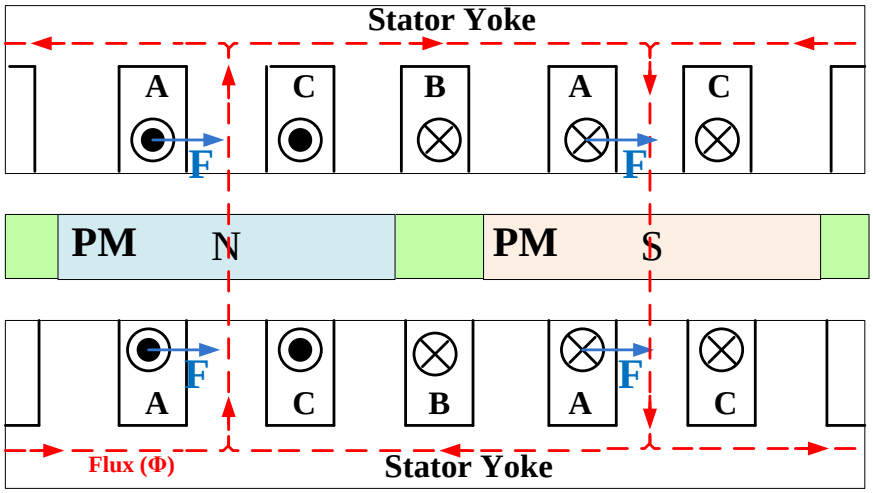

Figure 9. Axial-flux interior-rotor (AFIR) structure without steel disk.

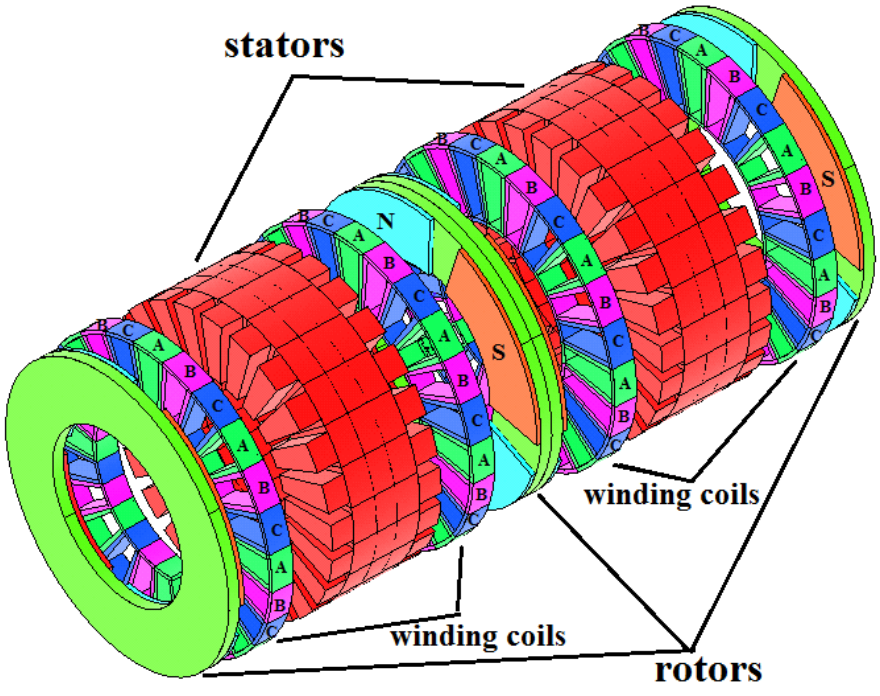

Figure 10. Multistage AFPM machine.

2000). Figure 12 shows an AFPM machine with variable-air-gap optimizing machine performance and allowing flux-weakening (Lipo and Aydin, 2004). It suits flux-weakening applications such as electric traction. The technique changes machine's torque constant, creating variable rotor and stator losses. Figure 13 shows AFPM machine torque-speed characteristic for various air-gaps. Uniqueness of axial flux enables air-gap variation, applicable also to single-stator double-rotor AFPM machines. The flux-weakening-capable AFPM machine in Profumo et al. (1998, 2000) that has two slotted stators and one rotor, uses soft magnetic materials (Figure 14). Core of the stator's slotted side is tape-wound, and the stator windings are series-connected. The rotor comprises disc, main poles, and leakage poles, and its magnets are axially magnetized. Between the main and the leakage poles are two flux barriers, whose appropriate designing gives the desired d-axis and q-axis

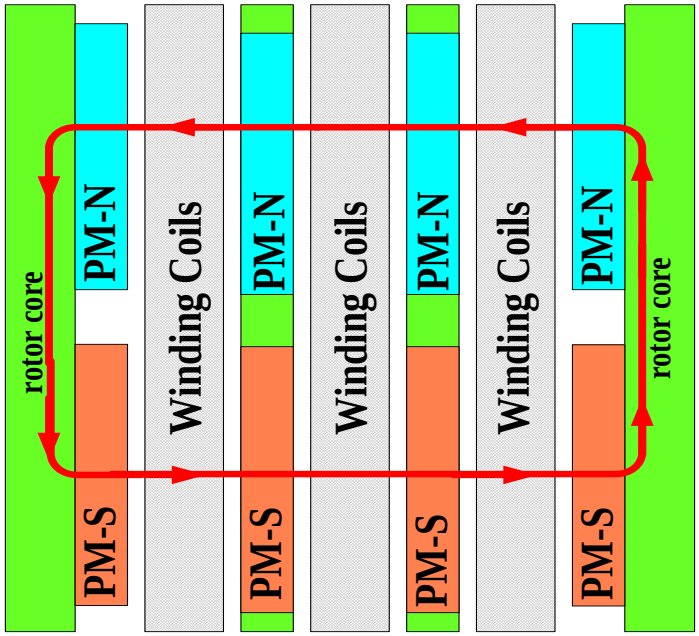

Figure 11. Multistage AFPM coreless stator machine.

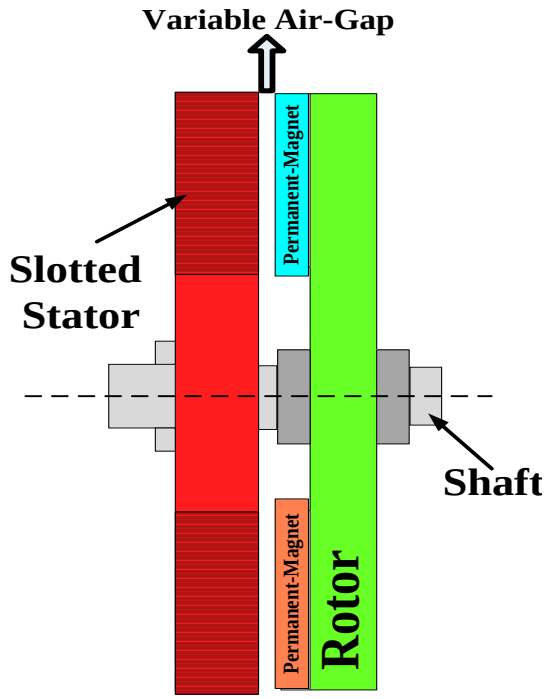

Figure 12. AFPM with variable air-gap and its torque-speed characteristic.

stator inductances in the flux-weakening region, for required torque. Figure 15 shows another type of AFPM machine with controllable flux. A field-weakening coil is used, its DC-current magnitude and polarity is controllable (Hsu, 2000). Machine structure is formed by two slotted stators with yoke, providing flux-return path and AC windings. Its rotor includes magnets and iron-pole pieces mounted on non-magnetic rotor body. Two toroidal field-weakening coils encircle shaft and frame, the latter made of mild steel to provide a flux path for the DC coils.

Figure 16 is another AFPM machine that applies the same DC-field-coil principle (Liang and Miller, 2002). Its structure is the same as the one preceding, but its rotor has permanent magnets with pole portions. The rotor magnets generate a first magnetic flux, and consequent poles generate a second magnetic flux. The field coil varies the second magnetic flux so the machine produces controllable output voltage. Aydin et al. (2010) presents a field-controlled AFPM machine with single stator and dual rotors, proposing the simple idea of air-gap flux control (Figure 17). The idea can be applied to any AFPM machines with multiple stators and rotors. Two strip-wound stator rings, two sets of three-phase windings and circumferentially-wound DC-field-winding placed between two stator rings comprise the machine's stators. The machine's rotor comprises arc-shaped iron pieces (axially magnetized magnets mounted on the inner surface of two rotor disks). A rotor pole is actually half permanent-magnet, half iron piece; space between the magnet and the iron piece reduces leakage. Excitation of DC-field-winding in one polarity increases flux on inner and outer sides of rotor pole, strengthening magnetic field, increasing flux linkage of stator armature

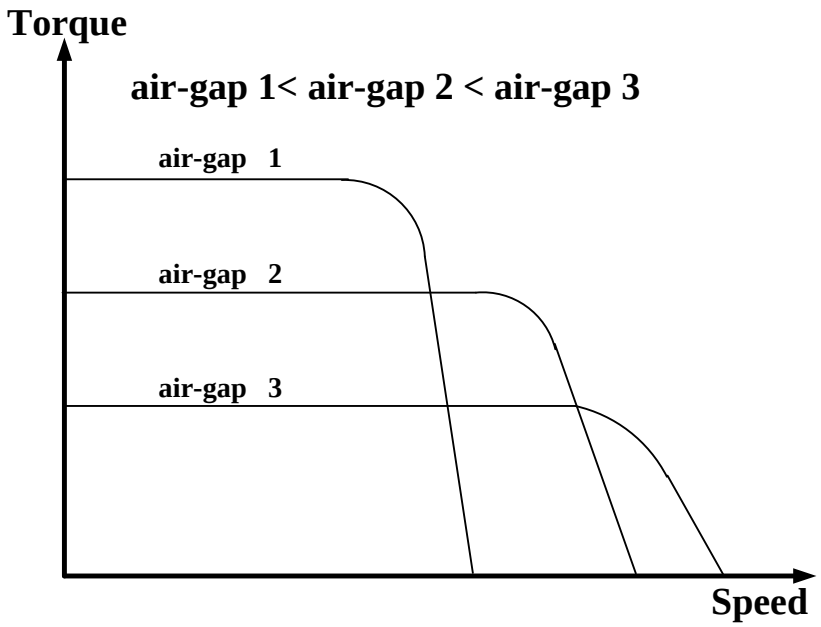

Figure 13. Torque-speed characteristic of a variable air-gap AFPM machine, for various air-gaps.

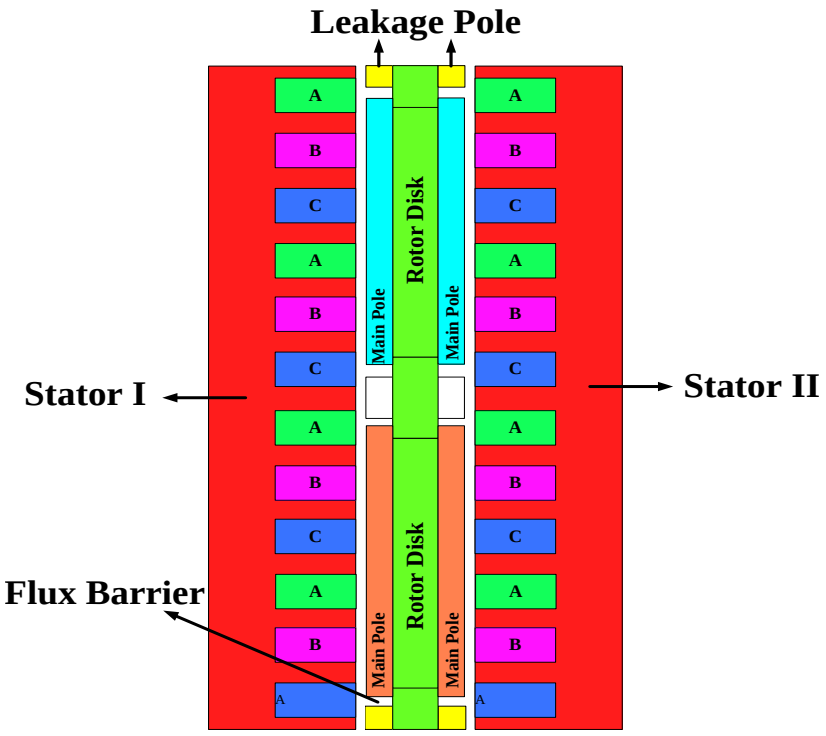

Figure 14. AFPM machine with soft magnetic materials.

windings. Excitation of opposite-polarity DC-field-winding decreases consequent-pole-flux in rotor-disc inner and outer sides, thus weakening field. Iron saturation and current density of DC-field limit flux boosting. Induced EMF thus increases or reduces according to DC excitation. If field winding is excited in the same direction

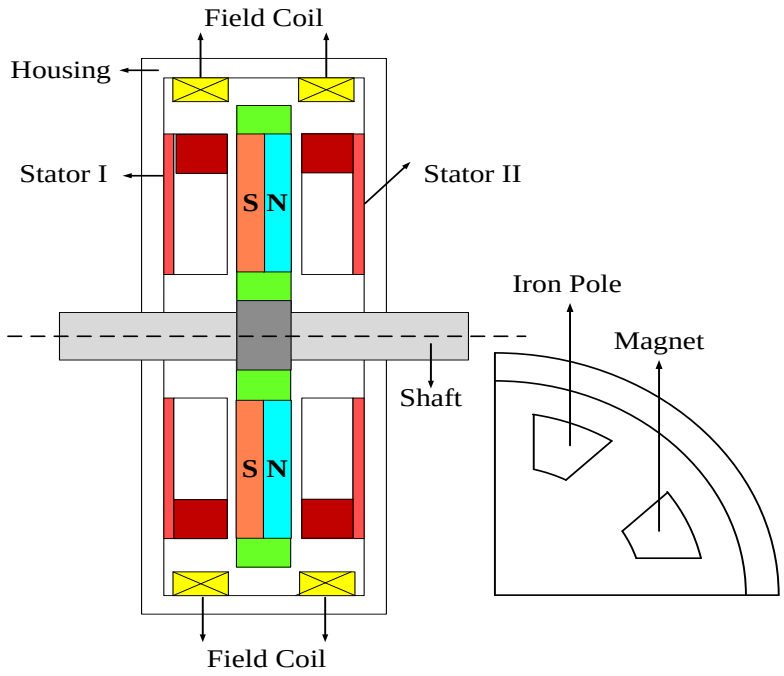

Figure 15. AFPM machine with direct control of air-gap-flux.

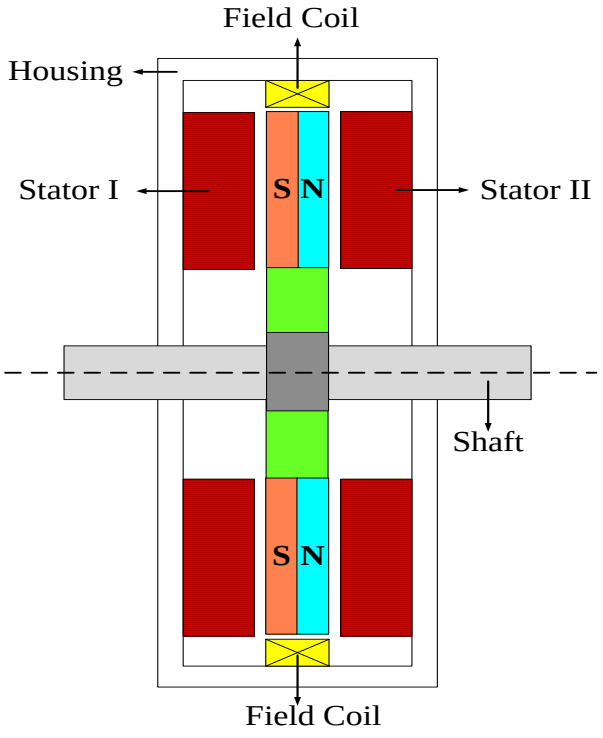

Figure 16. AFPM machine with flux control.

as the iron poles are, the machine becomes similar to a typical AFPM machine.

Modeling and simulation of the AFPM machine

Sizing equation for the AFPM machine

The design is in several steps. The first is to choose the configuration, that is, the number of phases, magnets and slots. Then, the main dimensions of each electrical machine are determined through electrical-machine-output power equation. Assuming negligible leakage inductance and resistance, rated power is expressed as:

$$P_{out} = \eta \frac{m}{T} \int_0^T e(t) \cdot i(t)\, dt \quad (1)$$

$e(t)$ is phase air-gap EMF, $i(t)$ is phase current, η is machine efficiency, m is number of machine phases and T period of one cycle EMF. A general-purpose sizing equation for AFPM machines has been provided by other authors previous literatures (Gholamian et al., 2008; Honsinger, 1980; Surong et al., 2001, 1998, 1999). For an AFPM machine, it takes the following form:

$$P_{out} = \frac{1}{1+K_\phi} \frac{m}{m_1} \frac{\pi}{2} K_e K_i K_p K_L \eta B_g A \frac{f}{P} (1-\lambda^2) \frac{1+\lambda}{2} D_1^2 L_e \quad (2)$$

m_1 is the number of each stator phase, K_e is EMF factor, Ki and K_p respectively are current and electrical power waveform factors, B_g is air-gap flux density, A is electrical loading total, D_1 is machine diameter on the

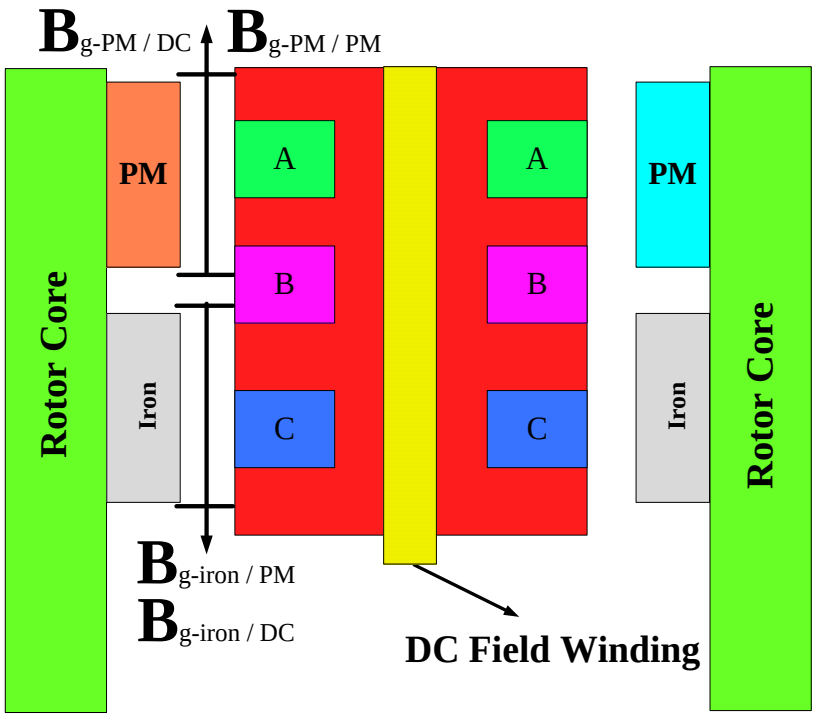

Figure 17. 2D cross-section of air-gap flux density components of field-controlled AFPM machine.

outer surfaces, $K_\varphi = A_r/A_s$ is electrical loading ratio, $K_L = D_1/L_e$ is aspect ratio coefficient for AFPM, and $\lambda = D_2/D_1$ is diameter ratio where D_2 is machine diameter on the inner surface. K_L pertinent to a specific machine structure is determined with considerations for effects of losses and temperature rise, and the design's efficiency requirements. Also, machine torque density for volume total is defined as:

$$\tau_{den} = \frac{P_{out}}{\omega_m \frac{\pi}{4} D_{tot}^2 L_{tot}} \quad (3)$$

ω_m is the rotor angular speed, D_{tot} and L_{tot} respectively are machine outer diameter total and machine length total including stack outer diameter and end-winding protrusion from radial and axial iron stacks. A procedure must be developed to select appropriate lengths for permanent-magnet, stator and rotor. Permanent-magnet length depends on air-gap length and air-gap flux density. Stator equivalent electrical loading, current density, slot-fill factor, and flux densities in various parts of the machine affect stator length and rotor length. Some literatures base on general-purpose sizing analysis, present optimization and design examples of AFPM machines (Gholamian et al., 2008; Honsinger, 1980; Surong et al., 1998, 1999, 2001). Air-gap flux density and diameter ratio are two important design parameters significantly affecting AFPM machine characteristics, so, for optimized machine performance, the parameters must be chosen carefully. From optimization-goal standpoint, diameter ratios vary; for specific flux density and electrical loading values, and various rated powers, pole pairs, converter frequencies, etc.

Field computation of the AFPM machine

Air-gap magnetic field determining AFPM machine performance can be calculated in several ways: analytical (Chan et al., 2009; Furlani, 1994; Kano et al., 2010; Lee, 1992; Loureiro et al, 2008; Qamaruzzaman and Dahono, 2008; Zhilichev, 1998), quasi 3D (Azzouzi et al., 2005; Kurronen and Pyrhonen, 2007; Marignetti et al., 2010), finite element method (FEM) (Bumby et al., 2004; Chan et al., 2010; Rong-Jie and Kamper, 2004; Upadhyay and Rajagopal, 2006), and method of images (Sang-Ho et al., 2006). FEM is more accurate than analytical method is, and can be used in complicated machine constructions. Finite element analysis (FEA) has long computation time, and a different model (including re-meshing) is needed when machine geometry changes. Shortfalls in early FEM were in meshing and in field-solving at rotor angles (causing

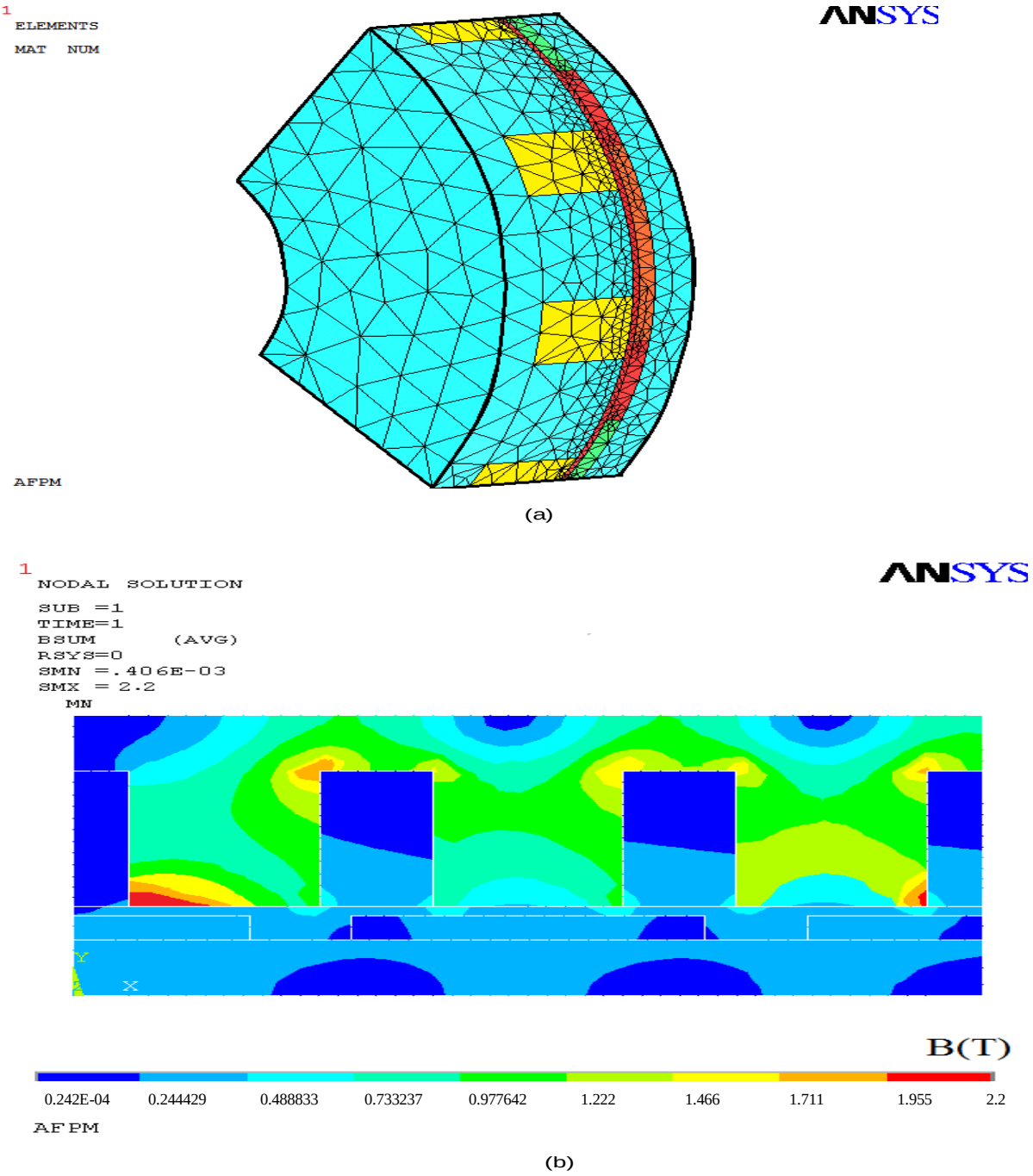

Figure 18. Field analysis of an AFPM machine, in ANSYS software; (a) 3D auto-mesh generation and (b) flux-density plot.

asymmetrical geometry, increasing complexity and 3D-field computation requirements). Sufficiently robust and mature automatic meshing and adaptive solution techniques that allow their routine use in FEA were then developed. Fully automated mesh preparation, boundary source and material data, equation solution, and machine-data extracted from solution thus allowed no prior knowledge of numerical analysis. Figure 18 is ANSYS field analysis of a single-sided AFPM machine (ANSYS 13.0, 2010; Mahmoudi et al., 2010). It shows the part used to model the machine. The structure includes 3 teeth and 1 pole-pair, fulfilling symmetry conditions. The machine comprises 12 slots and 4 pole-pairs. Figure 18a shows ANSYS software, a three-dimensional auto-mesh: tetrahedral elements with 6 nodes fitting circular shape of layers starting from shaft to outer diameter of AFPM

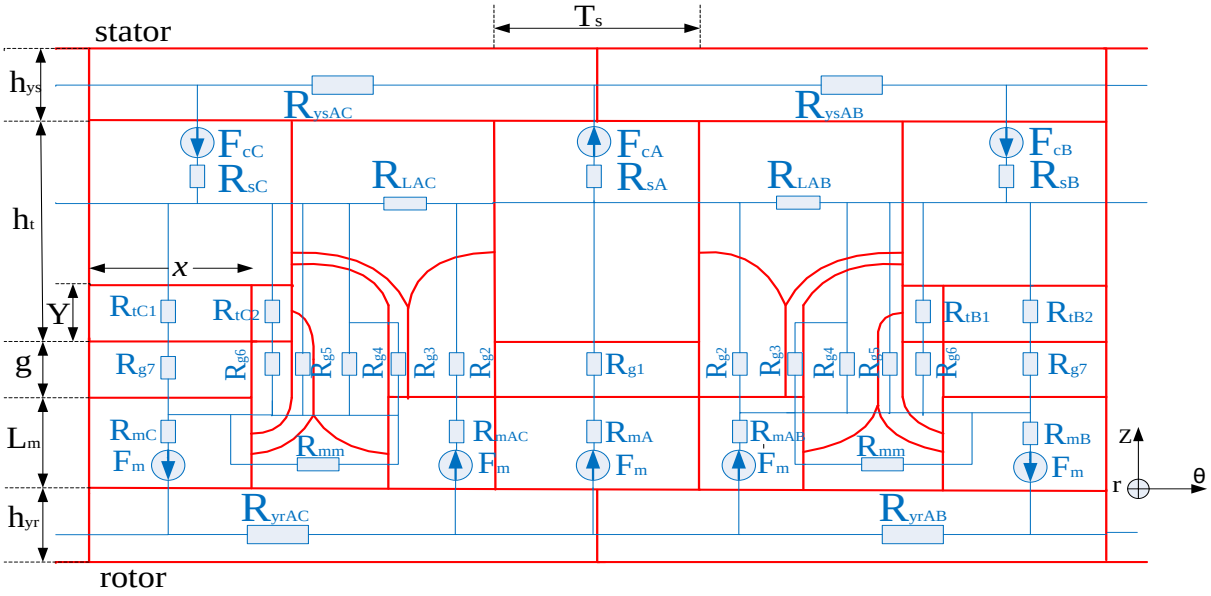

Figure 19. Magnetic-reluctance-network modeling of the AFPM machine.

machine. Figure 18b is axial distribution of its magnetic-flux density. More-adequate analytical models are based on two approaches: equivalent magnetic-reluctance network, and analytical resolution of Maxwell equations. The former is limited to simple cases as it usually needs conformal transformation to calculate air-gap magnetic-reluctance function. Maxwell-equation resolution gives all three magnetic-field components, so it is more accurate. Figure 19 is nonlinear-reluctance-based magnetic-reluctance network modeling of AFPM machine (Figure 18). All the methods can be implemented in 2D or 3D.

2D analysis of magnetic-field solution depends on ratio of air gap to pole pitch, the ratio varying with radius of the cylindrical cutting plane, so consideration of significant air-gap-flux density reduction at the inner and the outer circumferential regions is not possible. 2D field analysis cannot be applied when considering mutual and leakage fluxes in the end-winding regions, though it can handle fluxes along radial length of the active conductors. 2D analysis cannot account for changes in material properties in different cross sections, owing to considerable radial (as compared with axial) direction; 3D analysis is inevitable if precision is required. The analytical design tool used for quasi-3D computation is described in Marignetti et al. (2010). Figure 20 is transformation of the 3D model to corresponding 2D model used in quasi-3D computation. The machine is divided into *N* radial layers, each of thickness *W*. Average diameter of the *i*th layer ($D_{ave,\,i}$) is obtained from:

$$D_{ave,i} = D_2 + \frac{(D_1 - D_2)}{2 \times N} \times (2i - 1) \quad (4)$$

$$W = \frac{(D_1 - D_2)}{2 \times N} \quad (5)$$

If only air-space magnetic field is required, the method of images offers a straight forward and efficient solution (Sang-Ho et al., 2006), but the field in the magnets or in the iron core cannot be computed. To evaluate magnetic flux density distribution in an axial-flux machine's iron back plate, the 3D analytical model proposed by Hewitt et al. (2005) may be used. The method, however, assumes that magnetic flux enters core axially from air gap, and that the flux density is constant along radius, varying sinusoidally, circumferentially. Chan et al. (2010) shows that these assumptions are strictly not valid for the AFPM synchronous machine configuration being considered, particularly for rotor back plate with surface-mounted magnets. 3D FEA apparently has to be used if comprehensive machine study is required, as the method provides more precise modeling for machines with complicated geometries.

Analysis of the AFPM machine

Cogging torque analysis of AFPM machine

As conventional radial-flux do permanently-magnet machines, AFPM machines produce torque ripples, affecting output performance. Usual main sources of torque ripple are cogging torque, non-ideal back-EMF waveforms, saturation of machine magnetic circuit, and electronic-controller-induced. Ideal coreless-stator AFPM

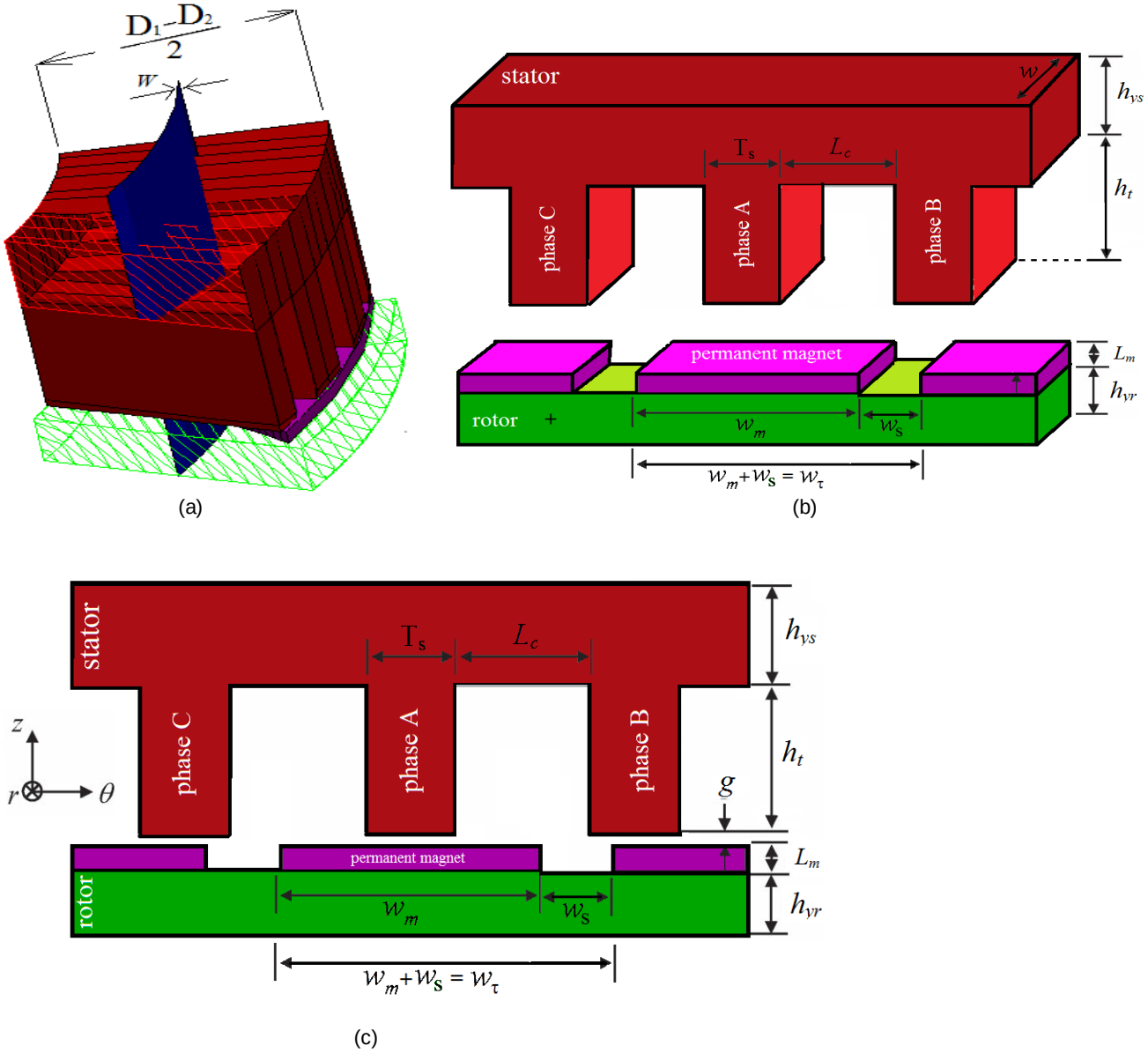

Figure 20. Transforming the AFPM machine's 3D geometry to 2D geometry, for use in quasi 3D computation. (a) Step 1: selecting computational plane of thickness W; (b) Step 2: On the selected computational plane, the AFPM's 3D geometry is transformed into linear-machine 3D geometry and (c) Step 3: Linear-machine 3D geometry reduced to 2D plane.

machine eliminates cogging torque. Parasitic torque ripples nevertheless exist, owing to machine design limitations and despite ideal controller. Techniques proposed to reduce torque ripple in RFPM machines include skewing of slots and magnets, magnet shaping and sizing, addition of dummy slots and control strategies. Recent attention in literatures is the analysis and reduction of cogging torque in AFPM machines (Caricchi et al., 2004; Fei et al., 2009; Mendrela and Jagiela, 2004; Virtic et al., 2008, 2009; Pisek, 2009); techniques to reduce cogging torque effect and torque development of AFPM machines with different structures were investigated, both theoretically and experimentally. Recent studies on torque reduction of AFPM machines propose many techniques to reduce cogging torque. Various techniques for minimizing cogging torque in AFPM machines were investigated by Aydin et al. (2007). A double-rotor, single-stator AFPM machine was used as reference machine and technique effectiveness was examined by 3D FEA. Letelier et al. (2007) present two methods (slot displacement and skewing) for cogging torque reduction in an axial, field-weakening-capable,

permanent-magnet machine (Letelier et al., 2007). Also, the influence of magnet shape was investigated by experiment in Gonzalez et al. (2007). The configuration analyzed was an AFPM machine with two rotors and double central stators. All the topologies allow introduction of displacement between both stator sides, reducing the resulting cogging torque. The study used FEA and 3D simulation. Hwang et al. (2009) used Taguchi method for reducing torque ripple in designing an AFPM machine with internal coreless stator and twin external permanent-magnet rotor, and well-established design procedures (Chang-Chou et al., 2009). It also describes improving the ratio between torque ripple and average torque.

Many AFPM machines have been optimally designed through FEA, but such analysis is generally time-consuming. Choi et al. (2009) applied the equation of magnetic flux lines existing between permanent-magnets; cores were assumed mathematically and the minimum cogging torque calculated theoretically and geometrically without finite element analysis (Jong-Hyun et al., 2009, 2009). The equation here is assumed as second-order polynomial. Calculation of skew angle minimizing cogging torque is theoretical. FEA and experiments confirm minimum-cogging-torque value.

Thermal analysis of the AFPM machine

Prediction of a new machine design's thermal performance traditionally according to parameters such as housing heat transfer coefficient, winding current density, or machine thermal resistance. Figures used for such parameters are estimated empirically from experiments on existing machines or from simple rules of thumb. Modern thermal analysis techniques are experiment, lumped-parameters thermal model and numerical analysis. Experiment method is appropriate for evaluation of cooling-strategy precise accuracy in designed and fabricated machines (Parviainen, 2004; Di-Gerlando et al., 2008; Marignetti et al., 2008, 2008; Sahin and Vandenput, 2003; Scowby et al., 2004; Sugimoto et al., 2007). Lumped-circuit analysis depicts thermal problem through a thermal network similar to an electrical circuit (Parviainen, 2005; Sahin and Vandenput, 2003). A thermal network in steady state comprises thermal resistance and heat sources connected between motor component nodes. For transient analysis, thermal capacitances are also used to consider change in body internal energy with time. Scowby et al. (2004) proposes a detailed lumped parameter thermal model, for prediction of transient and of steady-state temperature rise at various AFPM machine parts; it helps resize the motor (Scowby et al., 2004). Numerical methods (which are usually FEA-based) require calculation of different operating losses generated in various regions and form heat sources in the thermal analysis. Marignetti et al. (2009), studied exhaustively thermal characteristics of AFPM machine by 3D FEA, obtained isothermal distribution, thermal flux plot and thermal gradients in various rotor positions, and further developed a procedure to simulate steady state and transient thermal characteristics of AFPM machine through knowledge (obtained through airflow analysis) of air-velocity distribution inside machine (Marignetti et al., 2008, 2009). Temperature analysis can also be through cascade procedure, which comprises coupled electric, magnetic and thermal analysis. A recent trend is towards AFPM machine capable of high heat-dissipation, made possible with liquid-nitrogen-cooled HTS armature windings (Sugimoto et al., 2007) and application of materials capable of delivering generated heat at increased expected temperature (Herrault et al., 2008).

Experiment method, though accurate, is limited to designed-and-constructed machines. Lumped-para--meters thermal model is analytical; it quickly estimates machine-temperature distribution. Accurate prediction prefers numerical methods (3D-coupled electric, magnetic, and thermal, analysis). 3D method, though complex, gives highly accurate results for thermal behavior of an electrical machine. Figure 21 shows various thermal-analysis methods in determining temperature zones in an AFPM motor (Marignetti et al., 2008).

Mechanical analysis of the AFPM machine

An electrical machine needs good magnetic and mechanical design. A magnet length can not be chosen without considering its centrifugal-force effect on overall design, or air-gap length without considering axial attractive forces' effect. Centrifugal forces acting on rotor and axial stator-rotor attractive forces resulting from interaction of permanent magnets and stator cores are two major forces to be considered in mechanical analysis of an AFPM machine. Creating safe various-speed operating conditions through mechanical stress analysis of rotor, and critical frequencies by means of modal analysis are also issues in AFPM design. Figure 22 shows deformation patterns of an AFPM machine's rotor at its Eigen-frequencies (Sahin, 2001). McMillan and Ault, (2010), Mueller et al. (2005) and Yicheng et al. (2004) describe analysis of AFPM machines in applications of circular plate, elastic beam and cylindrical shell theory (to calculate AFPM structural mass). Various AFPM-machine topologies for wind generator are compared in references, but only active mass of magnetic-circuit iron, copper in stator windings, and rotor permanent-magnets were used (McMillan and Ault 2010; Yicheng et al., 2004). Structural mass of an AFPM machine dominates mass total. Mueller et al. (2005) designed and discussed a series of AFPM generators

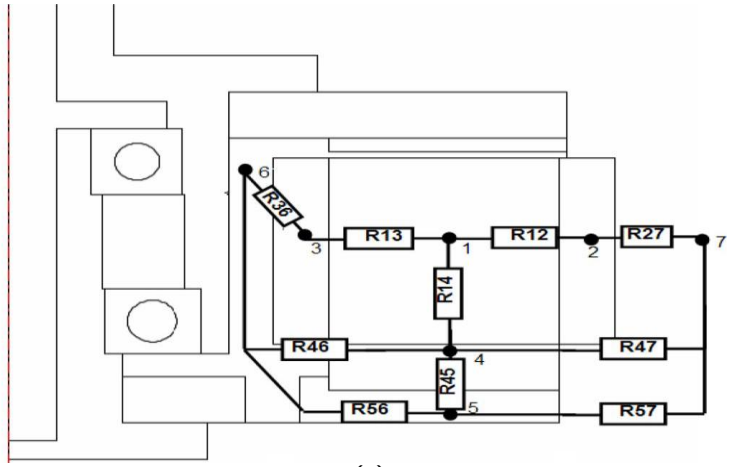

(a)

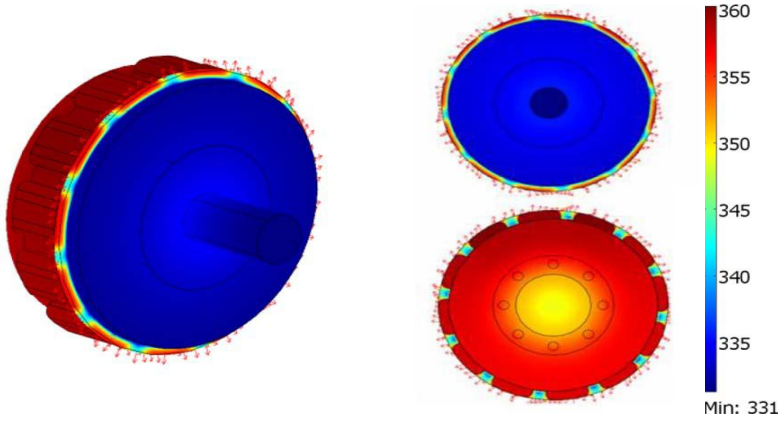

(b)

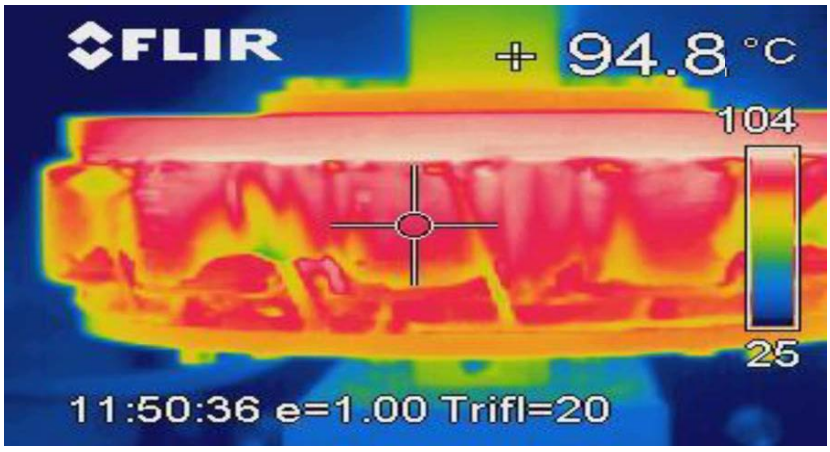

(c)

Figure 21. Thermal analysis of an AFPM motor through lumped-parameter thermal model, numerical analysis, and experiment; (a) equivalent thermal network of an AFPM machine; (b) temperature field via 3D finite element method and (c) temperature field from infrared image of an AFPM test-machine.

directly driven by wind turbines, demonstrating the importance of including structural mass analysis. The work's focus is double-rotor, single-stator configuration with/without iron in stator. AFPM machines also require

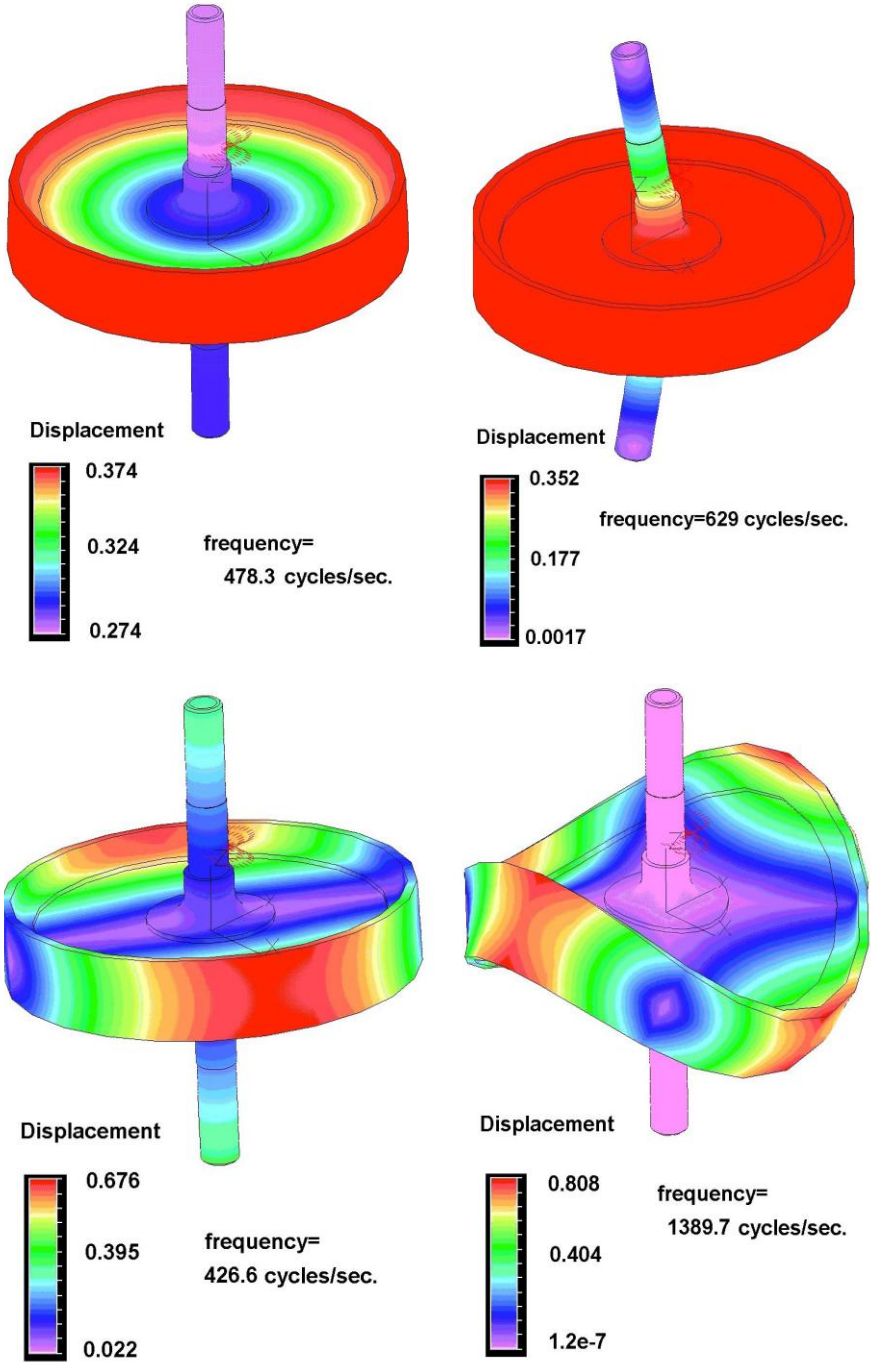

Figure 22. Deformation patterns of an AFPM machine's rotor at its Eigen-frequencies.

special materials to ensure machine performance but material choice in machines with stator core has not been much investigated. A first attempt was application of iron-powder resin as wedge in machine armature (Nafisi and Campbell, 1985). Sharkh and Mohammad, (2007) then investigated performance of two AFPM machines through use of powder iron and lamination steel materials as armature teeth (Sharkh and Mohammad, 2007).

Lee (1992) compared by experiment, electromagnetic and mechanical characteristic of a slotless AFPM machine according to use of spiral or lamination stator, such as phase back-EMF, core losses, frequency response function (FRF) characteristic, resonant frequency and

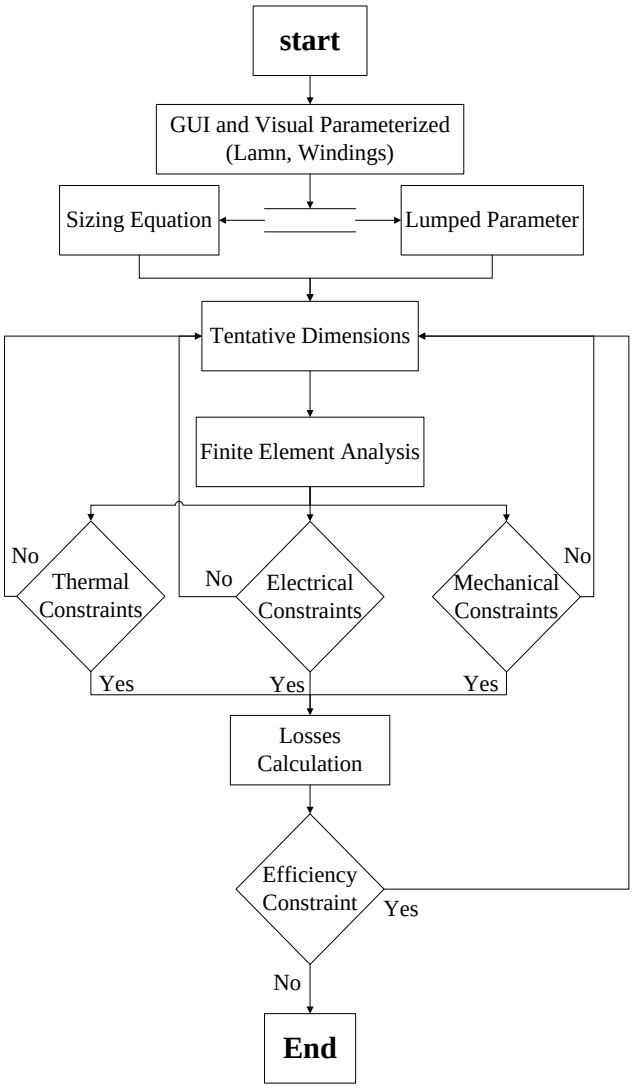

Figure 23. Basic structure of the design procedure.

sound pressure level (SPL) (Sang-Ho et al., 2009). Performance and iron losses of AFPM machine via use of non-oriented (NO) steel, with performance-enhancing and iron-loss-enhancing grain-oriented (GO) material (Kowal et al., 2010) was recently compared in FEA.

Design procedures of the AFPM machine

The design procedure of an AFPM machine is a multi-dimensional optimization problem in maximizing efficiency within constraints. Figure 23 shows the overall design methodology, which combines classical circuit model and directly finite element field solutions. The general optimization process adopted for an AFPM machine can be attempted under shape modification through choice of geometrical parameter, deterministic methods, or soft computing methods. Trade-offs is observed in all the shape-modification methods, among performance parameters such as torque ripple and obtainable average torque. Deterministic methods use numerical optimization procedure to optimize parameters. They are gradient-based methods that produce fast convergence in close-to-real-value initial estimation. Non-compliance to this condition leads to non-convergence. Another disadvantage is the tendency of deterministic methods to get stuck in local optimum points. Soft computing methods are based on artificial intelligence techniques; fuzzy logic, neural networks, evolutionary algorithm, and/or a combination of them. Heuristic, probabilistic methods that require good initial estimation, they give global optimum values and are highly pliable to multi-objective optimization problems. Long computation time for a solution and validity of the solution's accuracy are main disadvantages of the methods. Highly effective computer systems, new algorithms with fast computation, and highly efficient software packages, result in soft computing methods as present-day choices for optimization of AFPM machines.

AFPM applications

AFPM machines have for some years been used in various applications, most prominent of which are wind generator and electric vehicle. Direct-drive generator systems for wind turbines are considered better than geared generator systems, in terms of energy yield, reliability and maintenance (Li et and Chen, 2009). Direct-drive generator operates at low speed, so for large direct-drive wind turbines, a generator with high tangential force and large air-gap diameter is required (Chan et al., 2007). These requirements lead to heavy and expensive large direct-drive wind generators (Curiac et al., 2007; Polinder et al., 2006). Cost-effectiveness of large direct-drive generators for wind turbines is thus important. AFPM machine possibility and potential for large-scale direct-drive wind turbines have been discussed. Parviainen (2005) and Yicheng et al. (2005) present various surface-mounted permanent-magnet AFPM-machine structures. Jensen et al. (1992), Wei et al. (1995) and Wu et al. (1995) describe advantages of TORUS configuration as wind generator, and discuss its design procedure. Spooner and Chalmers, (1988) proposes low-speed direct-drive AFPM synchronous machine for 100 kW wind turbine, considering both mechanical and electromagnetic designs. Rossouw (2009), Sang-Ho et al. (2006) and Soderlund et al. (1996) describe design and development of an AFPM generator for direct-drive generator with small-scale wind turbine. AFPM generators with air-cored stator winding have recently become popular. Air-core windings are kept in position by epoxy resin rather than within iron slots.

Absent stator teeth and back-iron yoke mean no cogging torque and no iron losses. This type of AFPM generator is considered a high-efficiency machine (Kamper et al., 2008; Rong-Jie et al., 2005). Coreless AFPM generators have relatively low internal phase inductance, which may cause severe problems in noise and maximum power matching. Brisset et al. (2008) discuss a 9-phase, 2.7 MW AFPM generator with two permanent-magnet outer rotors and one interior 9-phase stator. They also present a comparative study of various-configuration 9-phase concentrated winding AFPM synchronous generator for direct-drive wind turbines. Ferraro et al. (2006) investigated flux-linkage regulation in a range of speeds for wind AFPM generator.

The concept of an in-wheel motor in electric vehicles appeared in the 1990s; the past twenty years saw attempts at designing many types of motors. Caricchi et al. (1996) developed a slotless AFPM motor as an in-wheel motor in an electric scooter. Slotless stator, however, has limited application in traction where motor is subjected to several types of stresses (Profumo et al., 1997). Johansen et al. (2001) discussed application of AFPM machine in-wheel direct drive in an electric bicycle, concentrating on electronic converter. Use of AFPM motors as in-wheel motors has in the last decade been more and more studied. Liu and Chuang (2002) presented systematic guidance for designing of an axial-flux disc-type surface-mounted permanent-magnet motor with single-sided stator windings (Cheng-Tsung et al., 2002). The motor was intended to motorize an electric scooter. Cheng et al. (2003) then presented field-oriented control of AFPM motor in electric vehicle. Yee-Pien et al. (2004), proposed systematic optimal design methodology for AFPM motor in-wheel motor and its drive for electric vehicles. Vehicle performance with the AFPM motor was in the same year simulated and tested by Sun et al. (2004) who based it on developed motor and controller model. Upadhyay et al. (2004) investigated the design of a compact winding for an AFPM machine used in an electric tow-wheeler. AFPM motor with a magnetic bridge in shunt with each permanent-magnet pole was then introduced (X-Zhu, 2006). In this AFPM type, not only was stator lamination maintained, but effect of DC field flux on permanent-magnet flux was also amplified. Yang and Chuang (2007) presented an optimal design for small-electric-passenger-car in-wheel motor (Yang et al., 2007). The work designed an axial-flux sandwich-type disc motor; the rotor was embedded with NdFeB magnets and two stator plates.

An AFPM motor was recently designed with independent stators capable of variable alignment, which allowed field weakening through a controllable and variable generated-voltage constant (Shah et al., 2010). The feature is useful especially in vehicle traction motors of large constant-power/speed ratio, where gear changes are not needed and overall size of motor drive must be kept the smallest possible. Recent research shows viable trend in AFPM motor application in future electric and hybrid vehicles. Besides the applications discussed, AFPM machines are becoming popular in other industries. Caricchi et al. (1999) proposed a new AFPM machine topology to apply to ship propulsion; synchronous counter-rotation of two-stage AFPM motors. Such topology finds application in direct drive of two counter-rotating propellers, which may be used in ship propulsion systems to recover energy from rotational flow of main propeller slipstream. Eastham et al. (2002) proposed a novel direct-drive brushless AFPM machine for aircraft drive. Adjustable speed pump (Caricchi et al., 1998), direct drive elevator (Ficheux et al., 2001), micro-power generation (Holmes et al., 2005), induction heating genes (Caricchi et al., 2010), slim vortex pump (Guo-Jhih et al., 2009), and automobile alternator (Javadi et al., 2009, 2010) are other AFPM machine applications. Small AFPM machines with etched and PCB windings are becoming common in some applications (Banitsch et al., 1994; Mi-Ching and Liang-Yi, 2006, 2007).

CONCLUSION

Comprehensive literature reviews of AFPM technology status and improvement trends were presented. Application of AFPM generators in wind energy systems and AFPM motors in electric vehicles signifies the technology's contribution to energy saving and to combating environmental pollution. Attractive and novel AFPM-machine structures including flux-weakening capability were examined from various perspectives. Various technical aspects of principles, machine structures, modeling, simulation, analysis, design and features of AFPM past to present have been reviewed. Despite tremendous AFPM-machine technology development, a gap exists in industry application. Current research trend strives to fill the void by developing more-efficient and more-cost-effective machines. The paper presented the works of various eminent authors, in numerous experiments and simulation results related to uniqueness of various design-related issues, characterization and cogging-torque reduction.

Nomenclature: P_{out}, rated output power (W); η, machine efficiency; m, number of phases; $e(t)$, phase air-gap EMF (V); $i(t)$, phase current (A); T, period of one cycle EMF (second); K_{φ}, electrical loading ratio; K_e, EMF factor; K_i, current waveform factor; K_p, electrical power waveform factor; B_g, air-gap flux density (Wb/m^2); f, Frequency (Hz); A, total electrical loading (A); λ, diameter ratio; D_1, outer diameter of machine stator (m); D_2, inner diameter of machine stator (m); A_r, rotor electrical loading (A); A_s, stator electrical loading (A); K_L, aspect ratio coefficient; L_e, effective stack length (m);

D_{tot}, total outer diameter of machine (m); L_{tot}, total axial length of machine (m); ω_m, otor angular speed (Rad/s); τ_{den}, torque density (N.m/m^3); D_{ave}, average diameter of machine stator (m); N,total number of radial layers; l, number of layer; W, thickness of each radial layer (m); w_m, magnet width (m); g, air-gap length (m); P, number of pole pairs; h_{ys}, stator-yoke thickness (m); h_{yr}, rotor-yoke thickness (m); L_m, magnet length (m); L_c width of slot opening (m); R, magnetic reluctance (1/H); F, magneto-motive force (MMF) (A); T_s, stator-tooth width (m); w_s, distance between two adjacent magnet (m); w_r, full pole pitch (m); x, rotor displacement (m); Y, pole tip length (m); h_t, stator pole height (m); R_t, saturated magnetic reluctance (1/H); R_s, magnetic reluctance of stator tooth (1/H); R_{mm}, magnet leakage reluctance (1/H).

REFERENCES

ANSYS 13.0 (2010). Finite Element Simulation Software. ANSYS Inc. Canonsburg PA.

Anyuan C, Nilssen R, Nysveen A (2010). Performance Comparisons Among Radial-Flux, Multistage Axial-Flux, and Three-Phase Transverse-Flux PM Machines for Downhole Applications. IEEE Trans. Ind. Appl., 46(2): 779-789.

Aydin M, Huang S, Lipo TA (2001). Optimum Design and 3D Finite Element Analysis of Nonslotted and Slotted Internal Rotor Type Axial Flux PM Disc Machines. IEEE Conf. Power Engineering Society Summer Meeting. Cambridge. MA.

Aydin M, Huang S, Lipo TA (2010). Design, Analysis, and Control of a Hybrid Field-Controlled Axial-Flux Permanent-Magnet Motor. IEEE Trans. Ind. Elect., 57(1): 78-87.

Aydin M, Surong H, Lipo TA (2006). Torque Quality and Comparison of Internal and External Rotor Axial Flux Surface-Magnet Disc Machines. IEEE Trans. Ind. Elect., 53(3): 822-830.

Aydin M, Zhu ZQ, Lipo TA, Howe D (2007). Minimization of Cogging Torque in Axial-Flux Permanent-Magnet Machines: Design Concepts. IEEE Trans. Mag., 43(9): 3614-3622.

Azzouzi J, Barakat G, Dakyo B (2005). Quasi-3-D Analytical modeling of the magnetic Field of an Axial Flux Permanent-Magnet Synchronous Machine. IEEE Trans. Energy Conversion Actions. 20(4): 746-752.

Banitsch R, Belmans R, Stephan R (1994). Small Axial Flux Motor with Permanent Magnet Excitation and Etched Airgap Winding. IEEE Trans. Mag., 30(2): 592-594.

Boules N (1985). Prediction of No-Load Flux Density Distribution in Permanent Magnet Machines. IEEE Trans. Ind. Appl., IA-21(3): 633-643.

Brisset S, Vizireanu D, Brochet P (2008). Design and Optimization of a Nine-Phase Axial-Flux PM Synchronous Generator with Concentrated Winding for Direct-Drive Wind Turbine. IEEE Trans. Ind. Appl. 44(3): 707-715.

Bumby JR, Martin R (2005). Axial-Flux Permanent-Magnet Air-Cored Generator for Small-Scale Wind Turbines. IET J., 152(5): 1065-1075.

Bumby JR, Martin R, Mueller MA, Spooner E, Brown NL, Chalmers BJ (2004). Electromagnetic Design of Axial-Flux Permanent Magnet Machines. IET J., 151(2): 151-160.

Campbell P (1975). The Magnetic Circuit of an Axial Field D.C. Electrical Machine. IEEE Trans. Mag., 11(5): 1541-1543.

Campbell P, Rosenberg DJ, Stanton DP (1981). The Computer Design and Optimization of Axial-Field Permanent Magnet Motors. IEEE Trans. Power Apparatus Syst. PAS-100(4): 1490-1497.

Caricchi F, Capponi FG, Crescimbini F, Solero L (2004). Experimental Study on Reducing Cogging Torque and No-Load Power Loss in Axial-Flux Permanent-Magnet Machines with Slotted Winding. IEEE Trans. Ind. Appl., 40(4): 1066-1075.

Caricchi F, Crescimbini F, Honorati O (1998). Low-Cost Compact Permanent Magnet Machine for Adjustable-Speed Pump Application. IEEE Trans. Ind. Appl., 34(1): 109-116.

Caricchi F, Crescimbini F, Honorati O, Bianco GL, Santini E (1998). Performance of Coreless-Winding Axial-Flux Permanent-Magnet Generator with Power Output at 400 Hz, 3000 r/min. IEEE Trans. Ind. Appl., 34(6): 1263-1269.

Caricchi F, Crescimbini F, Honrati O (1999). Modular Axial-Flux Permanent-Magnet Motor for Ship Propulsion Drives. IEEE Trans. Energy Conversion. 14(3): 673-679.

Caricchi F, Crescimbini F, Mezzetti F, Santini E (1996). Multistage Axial-Flux PM Machine for Wheel Direct Drive. IEEE Trans. Ind. Appl., 32(4): 882-888.

Caricchi F, Crescimbini F, Santini E (1995). Basic Principle and Design Criteria of Axial-Flux PM Machines Having Counterrotating Rotors. IEEE Trans. Ind. Appl., 31(5): 1062-1068.

Caricchi F, Maradei F, De Donato G, Capponi FG (2010). Axial-Flux Permanent-Magnet Generator for Induction Heating Gensets. IEEE Trans. Ind. Elect., 57(1): 128-137.

Cavagnino A, Lazzari M, Profumo F, Tenconi A (2000). Axial Flux Interior PM Synchronous Motor: Parameters Identification and Steady-State Performance Measurements. IEEE Trans. Ind. Appl., 36(6): 1581-1588.

Cavagnino A, Lazzari M, Profumo F, Tenconi A (2002). A Comparison between the Axial Flux and the Radial Flux Structures for PM Synchronous Motors. IEEE Trans. Ind. Appl., 38(6): 1517-1524.

Chalmers BJ, Spooner E (1999). An axial-flux permanent-magnet generator for a gearless wind energy system. IEEE Trans. Energy Conversion. 14(2): 251-257.

Chan CC (1987). Axial-Field Electrical Machines - Design and Applications. IEEE Trans. Energy Conversion. EC-2(2): 294-300.

Chan TF, Lai LL (2007). An Axial-Flux Permanent-Magnet Synchronous Generator for a Direct-Coupled Wind-Turbine System., IEEE Trans. Energy Conversion, 22(1): 86-94.

Chan TF, Lai LL, Shuming X (2009). Field Computation for an Axial Flux Permanent-Magnet Synchronous Generator. IEEE Trans. Energy Conversion, 24(1): 1-11.

Chan TF, Weimin W, Lai LL (2010). Performance of an Axial-Flux Permanent Magnet Synchronous Generator from 3-D Finite-Element Analysis. IEEE Trans. Energy Conversion, 25(3): 669-676.

Chang-Chou H, Ping-Lun L, Chuang FC, Cheng-Tsung L, Kuo-Hua H (2009). Optimization for Reduction of Torque Ripple in an Axial Flux Permanent Magnet Machine. IEEE Trans. Mag., 45(3): 1760-1763.

Cheng-Tsung L, Chiang TS, Zamora JFD, Lin SC (2003). Field-Oriented Control Evaluations of a Single-Sided Permanent Magnet Axial-Flux Motor for an Electric Vehicle. IEEE Trans. Mag., 39(5): 3280-3282.

Cheng-Tsung L, Kun-Chin C (2002). On the Design of a Disc-Type Surface-Mounted Permanent Magnet Motor for Electric Scooter Application. IEEE Conf. Industry Applications. 37th IAS Annual Meeting. 1(1): 377-383.

Curiac P, Do-Hyun K (2007). Preliminary Evaluation of a Megawatt-Class Low-Speed Axial Flux PMSM with Self-Magnetization Function of the Armature Coils. IEEE Trans. Energy Conversion, 22(3): 621-628.

Del Ferraro L, Caricchi F, Capponi FG (2006). Analysis and Comparison of a Speed-Dependent and a Torque-Dependent Mechanical Device for Wide Constant Power Speed Range in AFPM Starter/Alternators. IEEE Trans. Power Elect., 21(3): 720-729.

Di-Gerlando A, Foglia G, Perini R (2008). Permanent Magnet Machines for Modulated Damping of Seismic Vibrations: Electrical and Thermal Modeling. IEEE Trans. Ind. Elect., 55(10): 3602-3610.

Eastham JF, Profumo F, Tenconi A, Hill-Cottingham R, Coles P, Gianolio G (2002). Novel Axial Flux Machine for Aircraft Drive: Design and Modeling. IEEE Trans. Magnetics. 38(5): 3003-3005.

El-Hasan TS, Luk PCK, Bhinder FS, Ebaid MS (2000). Modular Design of High-Speed Permanent-Magnet Axial-Flux Generators. IEEE Trans. Magnetics, 36(5): 3558-3561.

Fei W, Luk PCK (2009). An Improved Model for the Back-EMF and Cogging Torque Characteristics of a Novel Axial Flux Permanent Magnet Synchronous Machine With a Segmental Laminated Stator.

IEEE Trans. Magnetics, 45(10): 4609-4612.
Ficheux RL, Caricchi F, Crescimbini F, Honorati O (2001). Axial-Flux Permanent-Magnet Motor for Direct-Drive Elevator Systems without Machine Room. IEEE Trans. Industry Applications. 37(6): 1693-1701.
Furlani EP (1994). Computing the Field in Permanent-Magnet Axial-Field Motors. IEEE Trans. Magnetics. 30(5): 3660-3663.
Gholamian S, Ardebili M, Abbaszadeh K (2008). Analytic and FEM Evaluation of Power Density for Various Types of Double-Sided Axial Flux Slotted PM Motors. Int. J. Appl. Eng. Res., 3(6): 749-762.
Gieras JF, Wang RJ, Kamper MJ (2008). Axial Flux Permanent Magnet Brushless Machines. Springer Verlag.
Gieras JF, Wing M (2002). Permanent Magnet Motor Technology: Design and Applications. CRC.
Gonzalez DA, Tapia JA, Bettancourt AL (2007). Design Consideration to Reduce Cogging Torque in Axial Flux Permanent-Magnet Machines. IEEE Trans. Magnetics. 43(8): 3435-3440.
Guo-Jhih Y, Liang-Yi H, Jing-Hui W, Mi-Ching T, Xin-Yi W (2009). Axial-Flux Permanent Magnet Brushless Motor for Slim Vortex Pumps. IEEE Trans. Magnetics. 45(10): 4732-4735.
Herrault F, Arnold DP, Zana I, Galle P, Allen MG (2008). High Temperature Operation of Multi-Watt Axial-Flux, Permanent-Magnet Microgenerators. Sensors and Actuators A: Physical, 148(1): 299-305.
Hewitt AJ, Ahfock A, Suslov SA (2005). Magnetic Flux Density Distribution in Axial Flux Machine Cores. IET J., 152(2): 292-296.
Holmes AS, Hong G, Pullen KR (2005). Axial-Flux Permanent Magnet Machines for Micropower Generation. J. Microelectromech. Syst., 14(1): 54-62.
Honsinger VB (1980). Performance of Polyphase Permanent Magnet Machines. IEEE Trans. Power Apparatus Syst. PAS-99(4): 1510-1518.
Hosseini SM, Agha-Mirsalim M, Mirzaei M (2008). Design, Prototyping, and Analysis of a Low Cost Axial-Flux Coreless Permanent-Magnet Generator. IEEE Trans. Magnetics. 44(1): 75-80.
Hsu JS (2000). Direct Control of Air-Gap Flux in Permanent-Magnet Machines. IEEE Trans. Energy Conversion. 15(4): 361-365.
Hsu JS (2000). Direct control of air gap flux in permanent magnet machines. United States Patent. No. 6057622.
Jahns TM (1987). Flux-Weakening Regime Operation of an Interior Permanent-Magnet Synchronous Motor Drive. IEEE Trans. Industry Applications. IA-23(4): 681-689.
Jang GH, Chang JH (2002). Development of an Axial-Gap Spindle Motor for Computer Hard Disk Drives Using PCB Winding and Dual Air Gaps. IEEE Trans. Magnetics, 38(5): 3297-3299.
Javadi S, Mirsalim M (2009). A Coreless Axial-Flux Permanent-Magnet Generator for Automotive Applications. IEEE Trans. Magnetics, 44(12): 4591-4598.
Javadi S, Agha-Mirsalim M (2010). Design and Analysis of 42-V Coreless Axial-Flux Permanent-Magnet Generators for Automotive Applications. IEEE Trans. Magnetics, 46(4): 1015-1023.
Jee IH (2008). AFPM Coreless Multi-Generator and Motor. United States Patent. No. 2008/091/035.
Jensen CC, Profumo F, Lipo TA (1992). A Low-Loss Permanent-Magnet Brushless DC Motor Utilizing Tape Wound Amorphous Iron., IEEE Trans. Industry Applications. 28(3): 646-651.
Johansen PR, Patterson D, O'Keefe C, Swenson J (2001). The Use of an Axial Flux Permanent Magnet In-Wheel Direct Drive in an Electric Bicycle. J. Renewable Energy, 22(1-3):151-157.
Jong-Hyun C, Jung-Hoon K, Dong-Ho K, Yoon-Su B (2009). Design and Parametric Analysis of Axial Flux PM Motors with Minimized Cogging Torque. IEEE Trans. Magnetics, 45(6): 2855-2858.
Jong-Hyun C, Yoon-Su B (2009). Theoretical Analysis and Its Applications of a PM Synchronous Motor with Minimized Cogging Force. IEEE Trans. Magnetics, 45(10): 4692-4695.
Kamper MJ, Rong-Jie W, Rossouw FG (2008). Analysis and Performance of Axial Flux Permanent-Magnet Machine with Air-Cored Nonoverlapping Concentrated Stator Windings. IEEE Trans. Ind. Appl., 44(5): 1495-1504.
Kano Y, Kosaka T, Matsui N (2010). A Simple Nonlinear Magnetic Analysis for Axial-Flux Permanent-Magnet Machines. IEEE Trans. Ind. Electronics, 57(6): 2124-2133.
Kowal D, Sergeant P, Dupre L, Van-den-Bossche A (2010). Comparison of Nonoriented and Grain-Oriented Material in an Axial Flux Permanent-Magnet Machine. IEEE Trans. Magnetics. 46(2): 279-285.
Kurronen P, Pyrhonen J (2007). Analytic Calculation of Axial-Flux Permanent-Magnet Motor Torque. IET J., 1(1): 59-63.
Lee JK (1992). Measurement of Magnetic Fields in Axial Field Motors. IEEE Trans. Mag., 28(5): 3021-3023.
Letelier AB, Gonzalez DA, Tapia JA, Wallace R, Valenzuela MA (2007). Cogging Torque Reduction in an Axial Flux PM Machine via Stator Slot Displacement and Skewing. IEEE Trans. Ind. Appl., 43(3): 685-693.
Leung WS, Chan JCC (1980). A New Design Approach for Axial-Field Electrical Machines. IEEE Trans. Power Apparatus Syst. PAS-99(4): 1679-1685.
Li H, Chen Z (2009). Design Optimization and Site Matching of Direct-Drive Permanent Magnet Wind Power Generator Systems. Renewable Energy, 34(4): 1175-1184.
Liang F, Miller JM (2002). Permanent Magnet Electric Machine with Flux Control. United States Patent. No. 6373162B1.
Lipo T, Aydin M (2004). Field Weakening of Permanent Magnet Machines–Design Approaches. EPE Power Electronics and Motion Control Conf. Riga, Latvia.
Liu CT, Lee SC (2006). Magnetic Field Modeling and Optimal Operational Control of a Single-Side Axial-Flux Permanent Magnet Motor with Center Poles. J. Mag. Mag. Mater., 304(1): 454-456.
Liu CT, Lin SC, Chiang TS (2004). On the Analytical Flux Distribution Modeling of An Axial-Flux Surface-Mounted Permanent Magnet Motor for Control Applications. J. Mag. Mag. Mater., 282: 346-350.
Locment F, Semail E, Piriou F (2006). Design and Study of a Multiphase Axial-Flux Machine. IEEE Trans. Mag., 42(4): 1427-1430.
Lombard N F, Kamper MJ (1999). Analysis and Performance of an Ironless Stator Axial Flux PM Machine. IEEE Trans. Energy Conversion, 14(4): 1051-1056.
Loureiro LTR, Filho AFF, Zabadal JRS, Homrich RP (2008). A Model of a Permanent Magnet Axial-Flux Machine Based on Lie's Symmetries. IEEE Trans. Mag., 44(11): 4321-4324.
Mahmoudi A, Rahim NA, Hew WP (2010). Analytical Method for Determining Axial-Flux Permanent-Magnet Machine Sensitivity to Design Variables. Int. Rev. Elect. Eng., (IREE). 5(5): 2039-2048.
Marignetti F, Colli VD (2009). Thermal Analysis of an Axial Flux Permanent-Magnet Synchronous Machine. IEEE Trans. Mag., 45(7): 2970-2975.
Marignetti F, Colli VD, Carbone S (2010). Comparison of Axial Flux PM Synchronous Machines With Different Rotor Back Cores. IEEE Trans. Mag., 46(2): 598-601.
Marignetti F, Delli-Colli V, Coia Y (2008). Design of Axial Flux PM Synchronous Machines Through 3-D Coupled Electromagnetic Thermal and Fluid-Dynamical Finite-Element Analysis. IEEE Trans. Ind. Elect., 55(10): 3591-3601.
McMillan D, Ault GW (2010). Techno-Economic Comparison of Operational Aspects for Direct Drive and Gearbox-Driven Wind Turbines. IEEE Trans. Energy Conversion, 25(1): 191-198.
Mendrela EA, Jagiela M (2004). Analysis of Torque Developed in Axial Flux, Single-Phase Brushless DC Motor with Salient-Pole Stator. IEEE Trans. Energy Conversion, 19(2): 271-277.
Mi-Ching T, Liang-Yi H (2006). Design of a Miniature Axial-Flux Spindle Motor with Rhomboidal PCB Winding. IEEE Trans. Mag., 42(10): 3488-3490.
Mi-Ching T, Liang-Yi H (2007). Winding Design and Fabrication of a Miniature Axial-Flux Motor by Micro-Electroforming. IEEE Trans. Mag., 43(7): 3223-3228.
Mueller MA, McDonald AS, Macpherson DE (2005). Structural Analysis of Low-Speed Axial-Flux Permanent-Magnet Machines. IET J., 152(6): 1417-1426.
Muljadi E, Butterfield CP, Yih-Huie W (1999). Axial-Flux Modular Permanent-Magnet Generator with a Toroidal Winding for Wind-Turbine Applications. IEEE Trans. Ind. Appl., 35(4): 831-836.
Nafisi A, Campbell P (1985). Composite Iron Powder Materials for the Armature of Axial-Field Permanent Magnet Machines. IEEE Trans. Mag., 21(5): 1753-1755.

Parviainen A, Pyrhönen MNJ (2004). Design of Axial-flux Permanent Magnet Machines: Thermal Analysis. Proc. Conf. International Conference on Electrical Machines (ICEM). Cracow, Poland.
Parviainen A (2005). Design of Axial-Flux Permanent-Magnet Low-Speed Machines and Performance Comparison between Radial-Flux and Axial-Flux Machines. PhD Dissertation, Dept. Elect. Eng., Lappeenranta University of Technology, pp. 16-25.
Parviainen, A, Niemela, M, Pyrhonen J (2004). Modeling of Axial Flux Permanent-Magnet Machines. IEEE Trans. Ind. Appl., 40(5): 1333-1340.
Patterson D, Spee R (1995). The Design and Development of an Axial Flux Permanent Magnet Brushless DC Motor for Wheel Drive in a Solar Powered Vehicle. IEEE Trans. Ind. Appl., 31(5): 1054-1061.
Platt D (1989). Permanent Magnet Synchronous Motor with Axial Flux Geometry. IEEE Trans. Magnet., 25(4): 3076-3079.
Polinder H, van-der-Pijl FFA, de-Vilder GJ, Tavner PJ (2006). Comparison of Direct-Drive and Geared Generator Concepts for Wind Turbines. IEEE Trans. Energy Conversion. 21(3): 725-733.
Profumo F, Tenconi A, Zhang Z, Cavagnino A (1998). Novel axial Flux Interior PM Synchronous Motor Realized with Powdered Soft Magnetic Materials. IEEE Conf. 33rd IAS Annual Meeting. Louis, MO.
Profumo F, Tenconi A, Zhang Z, Cavagnino A (2000). Design and Realization of a Novel Axial Flux Interior PM Synchronous Motor for Wheel-Motors Applications. Electric Machines Power Syst., 28(7): 637-649.
Profumo F, Zheng Z, Tenconi A (1997). Axial Flux Machines Drives: a New Viable Solution for Electric Cars, IEEE Trans. Ind. Elect., 44(1): 39-45.
Qamaruzzaman AP, Dahono P (1997). Analytical Prediction of Inductances of Slotless Axial-Flux Permanent Magnet Synchronous Generator Using Quasi-3D Method. Int. J. Elect. Eng. Inf., 1(2): 115-125.
Rong-Jie W, Kamper MJ (2004). Calculation of Eddy Current Loss in Axial Field Permanent-Magnet Machine with Coreless Stator. IEEE Trans. Energy Conversion, 19(3): 532-538.
Rong-Jie W, Kamper MJ, Van-der-Westhuizen K, Gieras JF (2005). Optimal Design of a Coreless Stator Axial Flux Permanent-Magnet Generator. IEEE Trans. Mag., 41(1): 55-64.
Rossouw FG (2009) Analysis and Design of Axial Flux Permanent Magnet Wind Generator System for Direct Battery Charging Applications. Master Dissertation, Dept. Elect. And Electro. Eng. Stellenbosch Univ., pp. 22-38.
Sadeghierad M, Darabi A, Lesani H, Monsef H (2009). Rotor Yoke Thickness of Coreless High-Speed Axial-Flux Permanent Magnet Generator. IEEE Trans. Mag., 45(4): 2032-2037.
Sadeghierad M, Lesani H, Monsef H, Darabi A (2009). High-Speed Axial-Flux Permanent-Magnet Generator with Coreless Stator. IEEE Trans. Mag., 34(1): 63-67.
Sahin F (2001). Design and Development of an Axial-Flux Permanent-Magnet Machine. Ph.D. Dissertation, Dept. Elect. Eng.. Technische Univ. Eindhoven. pp. 166-172.
Sahin F, Vandenput A (2003). Thermal Modeling and Testing of a High-Speed Axial-Flux Permanent-Magnet Machine. COMPEL: Int. J. Comput. Math. Elect. Elect. Eng.,, 22(4): 982-997.
Sang-Ho L, Do-Jin K, Jung-Pyo H, Jun-Hong P (2009). Characteristic Comparison Between the Spiral and the Lamination Stator in Axial Field Slotless Machines. IEEE Trans. Mag., 45(10): 4547-4549.
Sang-Ho L, Su-Beom P, Soon OK, Ji-Young L, Jung-Jong L, Jung-Pyo H (2006). Characteristic Analysis of the Slotless Axial-Flux Type Brushless DC Motors Using Image Method. IEEE Trans. Mag., 42(4): 1327-1330.
Scowby S, Dobson R, Kamper M (2004). Thermal Modelling of an Axial Flux Permanent Magnet Machine. Appl. Therm. Eng., 24(2-3): 193-207.
Sebastiangordon T, Slemon GR (1987). Operating Limits of Inverter-Driven Permanent Magnet Motor Drives. IEEE Trans. Ind. Appl., IA-23(2): 327-333.
Shah NP, Hirzel AD, Baekhyun C (2010). Transmissionless Selectively Aligned Surface-Permanent-Magnet BLDC Motor in Hybrid Electric Vehicles. IEEE Trans. Ind. Elect., 57(2): 669-677.
Sharkh SMA, Mohammad MTN (2007). Axial Field Permanent Magnet DC Motor with Powder Iron Armature. IEEE Trans. Energy Conversion, 22(3): 608-613.
Sitapati K, Krishnan R (2001). Performance Comparisons of Radial and Axial Field, Permanent-Magnet, Brushless Machines. IEEE Trans. Industr. Appl., 37(5): 1219-1226.
Soderlund L, Eriksson JT, Salonen J, Vihriala H, Perala R (1996). A Permanent-Magnet Generator for Wind Power Applications. IEEE Trans. Mag., 32(4): 2389-2392.
Spooner E, Chalmers B (1988). Toroidally-Wound, Slotless, Axial-Flux, Permanent-Magnet, Brushless-DC Motors. International Conf. Electrical Machines (ICEM). Pisa. Italy
Spooner E, Chalmers BJ (1992). `TORUS': a Slotless, Toroidal-Stator, Permanent-Magnet Generator. IET J., 139(6): 497-506.
Sugimoto H, Tsuda T, Morishita T, Hondou Y, Takeda T, Togawa H (2007). Development of an Axial Flux Type PM Synchronous Motor with the Liquid Nitrogen Cooled HTS Armature Windings. IEEE Trans. Appl. Superconductivity, 17(2): 1637-1640.
Sung-Chul O, Emadi A (2004). Test and Simulation of Axial Flux-Motor Characteristics for Hybrid Electric Vehicles. IEEE Trans. Vehicul. Technol., 53(3): 912-919.
Surong H, Aydin M, Lipo TA (2001). Torque Quality Assessment and Sizing Optimization for Surface Mounted Permanent Magnet Machines. IEEE Conf. Industry Applications. 36th IAS Annual Meeting. Chicago, IL.
Surong, H, Aydin M, Lipo TA (2001). TORUS Concept Machines: Pre-Prototyping Design Assessment for Two Major Topologies. IEEE Conf. Industry Applications. 36th IAS Annual Meeting. Chicago, IL.
Surong H, Jian L, Leonardi F, Lipo TA (1998). A General Approach to Sizing and Power Density Equations for Comparison of Electrical Machines. IEEE Trans. Ind. Appl., 34(1): 92-97.
Surong H, Jian L, Leonardi F, Lipo TA (1999). A Comparison of Power Density for Axial Flux Machines Based on General Purpose Sizing Equations. IEEE Trans. Energy Conversion, 14(2): 185-192.
Takano H, Itoh T, Mori K, Sakuta A, Hirasa T. (1992). Optimum Values for Magnet and Armature Winding Thickness for Axial-Field permanent magnet brushless DC motors. IEEE Trans. Ind. Appl., 28(2): 350-357.
Upadhyay PR, Rajagopal KR (2006). FE Analysis and Computer-Aided Design of a Sandwiched Axial-Flux Permanent Magnet Brushless DC Motor. IEEE Trans. Mag., 42(10): 3401-3403.
Upadhyay PR, Rajagopal KR, Singh BP (2004). Design of a Compact Winding for an Axial-Flux Permanent-Magnet Brushless DC Motor Used in an Electric Two-Wheeler. IEEE Trans. Mag., 40(4): 2026-2028.
Virtic P, Pisek P, Hadziselimovic M, Marcic T, Stumberger B (2009). Torque Analysis of an Axial Flux Permanent Magnet Synchronous Machine by Using Analytical Magnetic Field Calculation. IEEE Trans. Mag., 45(3): 1036-1039.
Virtic P, Pisek P, Marcic T, Hadziselimovic M, Stumberger B (2008). Analytical Analysis of Magnetic Field and Back Electromotive Force Calculation of an Axial-Flux Permanent Magnet Synchronous Generator with Coreless Stator, IEEE Trans. Mag., 44(11): 4333-4336.
Weh H, Mosebach H, May H (1984). Design Concepts and Force Generation in Inverter-Fed Synchronous Machines with Permanent Magnet Excitation. IEEE Trans. Mag., 20(5): 1756-1761.
Wei W, Spooner E, Chalmers BJ (1995). Reducing Voltage Regulation in Toroidal Permanent-Magnet Generators by Stator Saturation. IEEE Conf. 17th Electrical Machines and Drives International Conference. Durham, UK.
Woolmer TJ, McCulloch MD (2006). Axial Flux Permanent Magnet Machines: A New Topology for High Performance Applications. IET Conf. Hybrid Vehicle. pp. 27-42.
Wu W, Spooner E, Chalmers BJ (1995). Design of Slotless TORUS Generators with Reduced Voltage Regulation. IET J., 142(5): 337-343.
X-Zhu MC (2006). A Novel Stator Hybrid Excited Doubly Salient Permanent Magnet Brushless Machine For Electric Vehicles. J. Elect. Eng. Technol., 1(1): 185-191.
Yang YP, Chuang DS (2007). Optimal Design and Control of a Wheel Motor for Electric Passenger Cars. IEEE Trans. Mag., 43(1): 51-61.
Yee-Pien Y, Jui-Ping W, Shang-Wei W, Yih-Ping L (2004). Design and Control of Axial-Flux Brushless DC Wheel Motors for Electric Vehicles-

Part II: Optimal Current Waveforms and Performance Test. IEEE Trans. Mag., 40(4): 1883-1891.
Yee-Pien Y, Yih-Ping L, Cheng-Huei C (2004). Design and Control of Axial-Flux Brushless DC Wheel Motors for Electric Vehicles-part I: Multiobjective Optimal Design and Analysis. IEEE Trans. Mag., 40(4): 1873-1882.
Yicheng C, Pillay P, Khan A (2005). PM Wind Generator Topologies. IEEE Trans. Ind. Appl., 41(6): 1619-1626.
Yicheng C, Pragasen P, Khan A (2004). PM Wind Generator Comparison of Different Topologies. IEEE Conf. Industry Applications. 39th IAS Annual Meeting. Seattle, WA, USA.
Zhang Z, Profumo F, Tenconi A, Santamaria M (1997). Analysis and Experimental Validation of Performance for an Axial Flux Permanent Magnet Brushless DC Motor with Powder Iron Metallurgy Cores. IEEE Trans. Mag., 33(5): 4194-4196.
Zhilichev YN (1998). Three-Dimensional Analytic Model of Permanent Magnet Axial Flux Machine. IEEE Trans. Mag., 34(6): 3897-3901.